FATE OF OIL SPILL DROPLETS EXPOSED TO RANDOM DISPLACEMENT WITH TURBULENT DIFFUSION SOLUTIONS

A Thesis

by

MEGHAN MARY DANIELS

Submitted to the Office of Graduate and Professional Studies of
Texas A&M University
in partial fulfillment of the requirements for the degree of

MASTER OF SCIENCE

Chair of Committee,	Scott Socolofsky
Committee Members,	James Kaihatu
	Kristen Thyng
Head of Department,	Sharath Girimaji

May 2019

Major Subject: Ocean Engineering

ABSTRACT

Shipping trade routes are seeing an influx of traffic due to the increase in American trade and the ice melt occurring in the Arctic. The global warming effect on the Arctic's ice has peaked interest for possible trade routes and a heightened source of oil and gas development. The need for oil spill models that include variable environmental conditions, such as those in the Arctic, is significant because of this increase in marine operations and increased risk for an oil spill.

The Texas A&M Oil Spill Calculator includes Lagrangian particle tracking for bubble or droplet time-average trajectory prediction through the water column that includes a combination of fate processes. These fate processes include dissolution, heat transfer, and advection equations. In this thesis, the oil spill calculator was modified to incorporate a random displacement model and empirical relationships for vertical turbulent diffusivity as a function of density gradient and free-surface wind stress to better predict oil droplet fate in shallow water. Surface wind is a proven cause of turbulent diffusivity, specifically in the uppermost layers of the ocean. Therefore, an empirical relationship for wind and turbulent diffusion is applied to the mixed layer depths and the random displacement solution for diffusion is applied throughout the model domain.

To test the new model algorithms in the Texas A&M Oil Spill Calculator, we apply the model to scenarios of oil blowouts and subsea spills in Alaska with varying environmental conditions and send the nearfield output to the General NOAA Operational Modeling Environment tool which further predicts the farfield trajectory. This developed modelling method presents an accurate simulation for hazardous spill response and emergency cleanup efforts in adverse weather conditions.

DEDICATION

Dedicated to my loving family.

For their unwavering support in this endeavor.

ACKNOWLEDGMENTS

I would like to express great appreciation to my advisor, Dr. Scott Socolofsky. His assistance in the writing and research of this thesis has been invaluable and his guidance during my time at Texas A&M University made my graduate experience much more enjoyable. I am pleased to have him as an advisor and a role model in my life.

I would like to give special thanks to Jonas Gros who contributed to the TAMOC scripts for GNOME coupling and was an invaluable resource on plume simulations in TAMOC. Guidance on GNOME was provided by Chris Barker and Jay Hennen and were vital to my education and understanding of oil spill modeling. I would also like to thank Dr. Hetland for his time and support, and Dr. James Kaihatu and Dr. Kristen Thyng for their assistance and membership on my thesis committee.

I would also like to thank my research group members, Binbin, Jonas, Inok, Byungjin, Soobum, and Alex, for their friendship, support, and ideas in this research.

Lastly, I am thankful for my support system: the love of my life, Ryan, and my parents, David and Colleen, for the unconditional support and belief in my ability to accomplish anything I set out to complete.

CONTRIBUTORS AND FUNDING SOURCES

Contributors

This work was supported by a thesis committee consisting of Dr. Scott Socolofsky (advisor) and Dr. James Kaihatu of the Department of Ocean Engineering and Dr. Kristen Thyng of the Department of Oceanography at Texas A&M University.

All other work conducted for the thesis was completed by the student, under the advisement of Dr. Scott Socolofsky of the Department of Ocean Engineering.

Funding Sources

Graduate study and research was supported by the United States Coast Guard with the Advanced Education program.

NOMENCLATURE

ADAC	Arctic Domain Awareness Center
ADCP	Acoustic Doppler Current Profiler
BPM	Bent Plume Model
CTD	Conductivity-Temperature-Depth
DBM	Discrete Bubble Model
GNOME	General NOAA Operational Modeling Environment tool
NOAA	National Oceanographic and Atmospheric Administration
ODE	Ordinary Differential Equation
PDF	Probability Density Function
SBM	Single Bubble Model
TAMOC	Texas A&M Oilspill Calculator

TABLE OF CONTENTS

Page

LIST OF FIGURES

FIGURE Page

LIST OF TABLES

TABLE Page

1. INTRODUCTION

Oil spill models are a highly utilized tool for efficient marine hazardous spill response and research, and model accuracy is imperative. Through modeling multiple spill scenarios with the ability to input oil type, amount of oil, ambient seawater properties, and weather conditions, contingency plans and effective clean-up procedures for hazardous spill response can be identified and improved.

1.1 Background

The research and development of oil spill models increased after the impact the Deepwater Horizon oil spill had on the environment. A total discharge of almost 5 million barrels of oil spilled into the Gulf of Mexico with response efforts that lasted over 87 days with multiple containment failures and a detrimental impact to the environment in addition to loss of life (U.S. National Commission on the BP Deepwater Horizon Oil Spill and Offshore Drilling, 2011). The Deepwater Horizon spill is a worst-case example of the potential harm an oil release at sea can cause to the environment but gives an important purpose to continuous development and improvement of already-existing oil spill calculators.

The ice melt occurring in the Arctic in addition to the increasing oil and gas production and transportation is creating more interest for possible trade routes and a heightened source of oil and gas development in the Arctic region (Bureau of Ocean Energy Management, 2018). In 2014, there was 2,028 hazardous spills reported and 284,729 total gallons of oil and hazardous substances spilled in the Arctic, off of Alaskan coasts. Out of the 2,028 spills, 33% were due to seal failure and 17% due to vessel rollovers and capsizes, with 94% of the total hazardous spills being over 100 gallons in volume (Alaska Department of Environmental Conservation, 2015). With these numbers in mind and an expected increase in vessel traffic and development of oil production, the Arctic's risk for oil spills is heightened and the need for an oil spill model that supports variable environmental conditions relevant to the Arctic, with diffusion and mixed layer analysis, is significant.

The Texas A&M Oil Spill Calculator (TAMOC) is a research modeling suite used to predict subsea oil and gas spills and is readily available from http://github.com/socolofs/tamoc. In this research, we consider the random and rapid mixing caused by turbulent diffusion that exists in the water column and the effect of surface winds on diffusive mixing in the upper ocean layer and apply it to the combination of fate processes used to predict oil droplet transport within a defined nearfield domain. These fate processes include dissolution, heat transfer, and advection equations. In this thesis, we will develop a random displacement simulation using empirical relationships and combine it with the existing transport process within TAMOC to improve the accuracy of trajectory results of Lagrangian particles representing oil.

NOAA utilizes its own trajectory simulation model known as the General NOAA Operational Modeling Environment (GNOME). GNOME predicts the spread and trajectory of an oil spill using three main data components; maps, spills, and movers and is readily available from https://github.com/NOAA-ORR-ERD/PyGnome (Zelenke et al., 2012). The movers apply random walk to forces from winds, currents, and diffusion. In this thesis, we utilize TAMOC's nearfield plume simulation output and use it as input for GNOME to obtain farfield trajectory results with different diffusion solutions to assess model sensitivity.

1.2 Objectives

The objective of this research is to develop, test, and compare the affects of applying different diffusion schemes for transport of oil droplets in varying winds and stratification to oil spill trajectory models. The primary model used in this research is TAMOC. In order to compare the effects of random walk diffusion and random displacement diffusion, TAMOC modules are modified to accommodate a diffusivity profile and a random displacement simulation. The modified TAMOC model is coupled with GNOME, where subsurface release is simulated in several scenarios to compare the difference in random walk diffusion and random displacement diffusion. This study recognizes the impact of a non-uniform, vertical diffusivity field in particle-tracking integral models.

2. EXISTING PLUME MODELS

TAMOC and GNOME are both oil spill modeling platforms which include Lagrangian particle tracking for oil trajectory modeling (Socolofsky et al., 2015; Zelenke et al., 2012). In this study, TAMOC is modified to be capable of adding diffusion to oil transport, GNOME already has this feature. GNOME utilizes a random walk simulation which assumes a uniform diffusivity field which has been proven unrealistic in the ocean water column due to the unlikelihood of a uniform diffusivity profile (Visser, 1997). In this thesis, we update TAMOC to apply the Visser scheme for random displacement simulation which considers a spatially varying diffusivity field and has proven to be a more accurate approach to applying diffusion (Gräwe, 2011; Visser, 1997).

2.1 TAMOC

TAMOC is a modeling suite developed by Dr. Scott Socolofsky of Texas A&M University and is coded in Python and Fortran. TAMOC predicts the fate of subsea oil and gas spills. The model was thoroughly validated with Deepwater Horizon oil spill data in addition to laboratory and field data (Gros et al., 2017; Dissanayake et al., 2018). TAMOC is comprised of three simulation models: the Single Bubble Model (SBM), Stratified Plume Model (SPM), and Bent Plume Model (BPM) with two modules designed to input and compute properties for every time step: the Ambient module and Discrete Bubble Model (DBM) (Socolofsky et al., 2015). In this study, we make changes that affect the SBM and BPM simulation modules.

2.1.1 Ambient Module

The ambient module is used to manipulate seawater CTD data by adjusting units, calculating other variables, and storing data in a NetCDF4 format. The module requires the input of temperature and salinity data which can come from CTD profilers and numerical simulations. The module also accepts directional current data, trace gas concentration data, and modeled hydrocarbons for inputted data (Dissanayake et al., 2018).

2.1.2 Discrete Bubble Model

The DBM applies the thermodynamic equations of state and computes fluid properties along the track of individual bubbles or droplets. The applied trajectory is then applied to a number of bubbles within the same plume, assuming they are identical. The properties defined in the DBM are both thermodynamic and physical, and these can be identified by TAMOC's description of hydrocarbon gas and liquid mixtures (Dissanayake et al., 2018).

2.1.3 Single Bubble Model

The SBM uses water properties from the ambient module and its defined CTD profile together with particle properties from the DBM to track a single bubble or droplet as it rises through a water column (Dissanayake et al., 2018). This module uses a combination of fate and transport processes to predict bubble trajectories within a defined nearfield domain. These processes include particle dissolution, heat transfer, and pure advection, which accounts for ambient currents and particle slip velocity.

Dissolution

Dissolution occurs when the soluble hydrocarbons in gas bubbles or oil droplets dissolve into the surrounding water column (Spaulding, 2017). Dissolution is evaluated differently for surface and subsurface models. TAMOC uses a Ranz-Marshall equation to compute individual particle dissolution (Dissanayake et al., 2018) which represents dissolution as a mass flux with respect to the particle's surface area and is expressed as:

$$\frac{dm_i}{dt} = -A\beta(C_s - C)_i \tag{2.1}$$

where m_i is the mass of an individual compound in the particle, A is the surface area of a droplet, β is the mass transfer coefficient, C is the ambient concentration, s is the solubility, and i indicates the individual compound.

Heat Transfer

The heat transfer of the oil particle is influenced by the ambient interface properties and the dispersed particle properties (Wegener et al., 2014). Heat transfer is modeled in TAMOC similarly to dissolution. Utilizing a heat transfer equation with respect to the difference in ambient temperature and the temperature of a droplet (Dissanayake et al., 2018). Once an oil droplet cools from its release condition to the temperature of the ambient water, heat transfer is no longer tracked, and the droplet is assumed to be in thermal equilibrium with the water.

Advection

Advection is the movement of an oil particle by the surrounding environmental forcing from wind, waves, and currents (Reed et al., 1999). Since TAMOC is a subsea oil spill calculator, only ambient seawater currents for advection are considered. TAMOC calculates advection of a particle by the sum of ambient seawater velocities and slip velocity of the particle, which is specific to the vertical direction using the following equation:

$$\frac{d\vec{x}}{dt} = \vec{u} + u_s\hat{k} \tag{2.2}$$

where $\vec{x}$ is the vector position of a droplet, $\vec{u}$ is the vector velocity of ambient seawater, u_s is the slip velocity of droplet relative to ambient seawater, and $\hat{k}$ refers to the vertical direction. Ambient currents are input to TAMOC and may come from measurements or model simulation output (Dissanayake et al., 2018).

2.1.4 Bent Plume Model

The BPM is a Lagrangian integral plume model exposed to crossflow currents and ambient density stratification (Dissanayake et al., 2018). The BPM provides the ability to track the location of particles inside and outside the plume of oil, gas, and entrained seawater while applying crossflow and ambient conditions. This model follows the approach of the Clarkson Deep Oil and Gas (CDOG) model (Zheng and Yapa, 1998) and the DeepBlow model (Johansen, 2000).

2.2 GNOME

GNOME is an oil spill model used by NOAA to forecast oil spill trajectories within hours of an accident. GNOME produces farfield image and movie forecasts that consider factors such as currents, windage, diffusion, and spreading for oil spills. GNOME begins with a map input and applies movers which are defined as any physics that cause movement to a particle in water (Zelenke et al., 2012). The movers defined in GNOME are wind, currents, and diffusion. These are superposed and applied to Lagrangian elements on the grid using a forward Euler scheme. The input for movers are Cartesian coordinates and time and the output is displacement at the elapsed time.

2.2.1 Spills

Spills are defined in GNOME as lagrangian elements where each element contains a position, depth, release time, and pollutant parameters. Each element also contains a status which can be either floating, beached, or evaporated (Zelenke et al., 2012).

Tamoc Spill

The Tamoc Spill script in GNOME is where the hand off from TAMOC to GNOME occurs. This script runs the Tblowout simulation in TAMOC for a nearfield trajectory and passes the particle locations at the end of the nearfield to GNOME where the farfield trajectory is completed for the same spill. This script defines inputs for the TAMOC model which inlude release time, initial position, and ambient seawater and plume parameters. Once the tamoc spill has run, the script updates tamoc elements to a list of gnome particles for GNOME to further evaluate the spill.

2.2.2 Diffusion

GNOME applies diffusion using Fick's Law and a random walk scheme and an assumed diffusivity value. The diffusion equation is expressed as,

$$\frac{dC}{dt} = \nabla(D\nabla C) \tag{2.3}$$

where C is the concentration of the particle and D is the diffusion coefficient, which defaults to 100,000 cm^2/s in GNOME (Zelenke et al., 2012). This equation is further simplified using Csanady (1973)'s characterization of particle displacement as a probability density function, where the mean position remains zero and the variance grows linearly with time in a Gaussian curve. In order to define the displacement of a particle from a reference location, we define the mean square distance or standard deviation as $\sigma_x^2 = 2D\Delta t = \frac{\Delta x^2}{3}$, where Δx is the particle displacement in the x-direction and is chosen randomly from a distribution. In GNOME, a uniform distribution is used, meaning the displacements in the x- and y-directions are equivalent in addition to the variance of the distribution for each direction. This relationship gives the following random walk equation for the x-direction and y-direction, assuming the diffusivities in the x- and y-directions are constant,

$$\Delta x = \sqrt{6D_x\Delta t}, \Delta y = \sqrt{6D_y\Delta t} \tag{2.4}$$

where D_x,D_y is the horizontal diffusivity and Δt is a time step.

2.2.3 Wind

Gnome allows three different methods for applying wind with wind movers: constant, time-dependent, and time/space dependent, which requires uploading wind files and interpolation. An alternative also used in GNOME is to load the wind as current files and utilize them at a fixed percentage, the default is 3 percent of the original wind speeds. GNOME uses a surface model of mixing that assumes when a particle reaches the surface it is exposed to wind for a default time step or persistence of 15 minutes and then reflects below the surface.

2.3 TAMOC-GNOME Coupling

The nearfield output from TAMOC is used as input for GNOME to obtain farfield results of the same spill scenario entered into TAMOC. Figure 2.1 is a visual of the coupling of TAMOC and GNOME, TAMOC evaluates a subsurface oil release in a nearfield domain by applying the fate and transport processes aforementioned to predict particle trajectory, once particles reach the end of buoyant effects and adjust to the currents, they are passed to GNOME to compute farfield

trajectory. The range for the nearfield domain is an input and may be altered to best describe specific simulations. In this thesis, we apply random displacement to TAMOC's advection process and analyze the differences from the previous advection scheme.

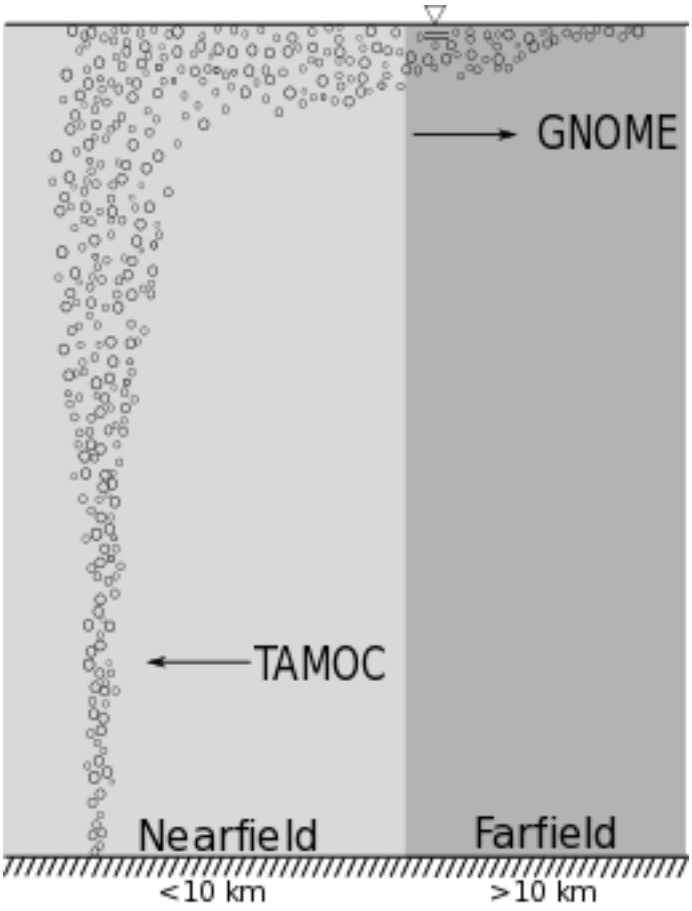

Figure 2.1: Diagram of TAMOC and GNOME coupling interaction.

3. LITERATURE REVIEW

With the increase in oil and gas movement in America since the 1980s, the need for accurate oil spill models is heightened with the potential risk of a spill (ABSG Consulting Inc., 2018). Existing models are constantly under development with improved methods and recent data. In order to accurately predict the trajectory of an oil spill, environmental fate processes need to be applied such as ambient conditions, slip velocity, heat transfer, and diffusion. There are multiple methods to defining and applying diffusion in numerical models. Solutions for defining a diffusivity profile may include variables such as depth, density profile, and surface wind.

An extensive literature review was conducted during this study to provide greater insight into predicting particle trajectories using Lagrangian models to handle diffusion with the application of random walk and random displacement. First, oil spill models are examined to better understand TAMOC and its application for subsea oil spills. Next, the transport and fate processes which affect oil particles in subsea spill scenarios are reviewed for modeling purposes, specifically turbulent diffusion. Lastly, the relationship between the density profile and wind on diffusion was studied with emphasis on finding empirical solutions that could be applied in numerical models.

3.1 Oil Spill Models

There are multiple ways oil can be released into a marine environment, some more common than others. The most frequent oil spill accidents occur from a vessel either sunken or ruptured, other methods include pipeline breaches, natural oil seeps in the ocean floor and well head failures (ABSG Consulting Inc., 2018). These spills can be modeled in the abundance of oil spill models in use today. Accurate models use different types of oil, the release flow rate, and environmental data for an efficient output.

Kileso et al. (2014) explains the general approach to an oil spill model as the combination of three main modules: an input module, a transport module, and a fate module. The input module includes the initial environmental and oil spill properties. The transport module calculates particle

drift by environmental forcing such as wind, currents, and waves. The fate module calculates the changes in oil mass and properties from individual fate processes such as evaporation, emulsification, and biodegradation (Kileso et al., 2014). The typical design of an oil spill model is shown in Figure 3.1.

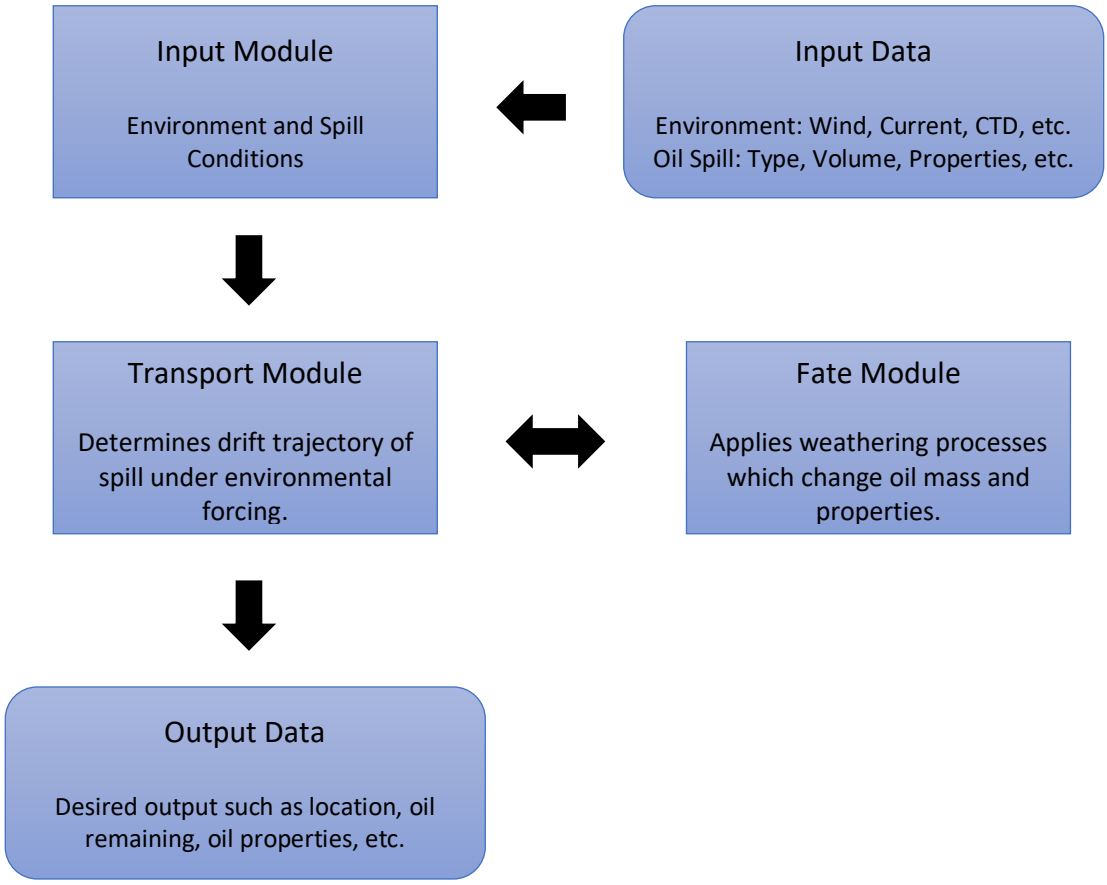

Figure 3.1: General design of oil spill models, figure modified from Kileso et al. (2014).

Expected required output of an oil spill model is the forecast or fate of an oil spill described by the spatial and temporal distribution of particles or droplets. Additional desired output is the remaining mass balance and change in properties of the oil after exposure to ambient conditions and weathering processes (ITOPF, 2019).

Particle Tracking Model

A particle tracking model identifies an oil spill as a mass of elements or particles. Each particle is defined by a location and parameters regarding diameter, mass, and oil type, then the particle's advection is calculated and exposed to environmental elements such as wind and current forcing (Díaz et al., 2008; Kileso et al., 2014).

3.2 Oil Trajectory

The primary processes that affect oil spill transport include spreading, evaporation, dissolution, entrainment, emulsification, biodegradation, and diffusion (Spaulding, 2017). When a subsurface spill occurs, oil and gas generate multi-phase plumes where entrainment occurs and droplets escape from the plume by ambient forces or remain in the plume from strong stratification (Socolofsky et al., 2008). When ambient currents are weak, stratification plays a dominant role and the plume becomes stratification-dominated (Dissanayake et al., 2018). Figure 3.2, courtesy of Spaulding (2017), depicts the fate processes with potential impact on oil particle transport and other surrounding factors to be considered.

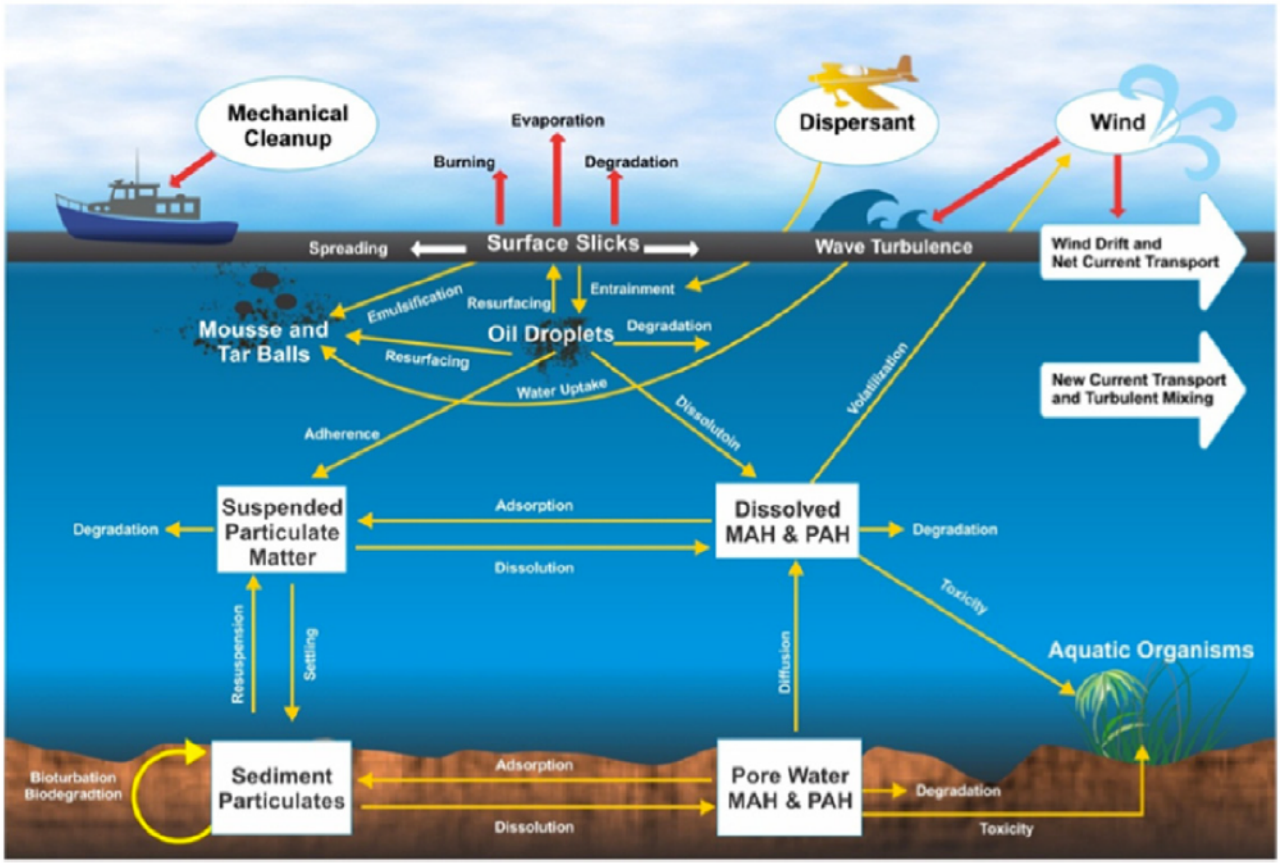

Figure 3.2: Oil fate processes in the open ocean reprinted with permission from "State of the art review and future directions in oil spill modeling." by Spaulding (2017).

3.2.1 Euler Trajectory Method

The Euler trajectory method is a first-order, forward estimation scheme for solutions to differential equations of the initial value type. Euler's method assumes a constant tangential slope over each step interval forward in order to predict solutions. This method is also referred to as the nonstationary diffusion equation for tracer approach, where diffusion equations define a particles transport (Kileso et al., 2014). This method is commonly used in modeling oil spill droplet trajectories in the farfield, such as GNOME. This approach is also used in the operational hybrid model, MEDSLIK-II (Dominicis et al., 2013). Euler's method is commonly used because it is a fast approach for a solution, but it is not very accurate compared to higher-order estimations (Press et al., 2007).

3.2.2 Lagrangian Trajectory Method

The Lagrangian approach is the most commonly used approach for calculating advection of oil spills. This approach assumes a Eulerian flow field and an oil spill made up of Lagrangian elements, therefore the particles have no effect on the flow field (Kileso et al., 2014). Models use this method to avoid numerical diffusion of Eulerian methods for oil transport on a course grid. This approach results in the need to solve a system of coupled, non-linear Ordinary Differential Equations (ODE) where the particle path is a function of location and time by advection, dissolution, and heat transfer. The system of equations computes the mean path for multiphase particles. Operational modes that successfully apply the Lagrangian approach for calculating oil spill advection include GNOME and TAMOC (Zelenke et al., 2012; Socolofsky et al., 2015).

ODE Solvers

The SciPy package of Python provides a variable-coefficient ODE solver. The ODE solver integrates a particle's path using backward differentiation formulas, this solver was previously used by TAMOC. TAMOC was modified to utilize the Runge-Kutta method, both second- and fourth-order, for solving the particle's path. The Runge-Kutta second-order method is similar to the Euler method but uses the initial derivative at each step to find a point halfway across the interval, then uses the midpoint derivative across the whole interval. The Runge-Kutta fourth-order method, which is the most commonly used, evaluates the derivative four times, at the initial point, twice at the halfway points, and once at the trial endpoint (Press et al., 2007). The Runge-Kutta method is a higher-order method, used because of its higher solution accuracy but can be time-consuming for computing a solution (Press et al., 2007).

3.3 Diffusion

Turbulent diffusion is commonly applied with a simple Euler scheme using a uniform diffusivity, which does not represent an accurate picture of the random dispersion which occurs in a marine environment because turbulent diffusivity in marine systems are most commonly spatially non-uniform (Visser, 1997). There are two solutions for the turbulent diffusion simulation, the

commonly used random walk model, Equation 3.1, and the diffusive random walk model or random displacement model, Equation 3.2. The differences being an additional non-random advective component that correlates with depths of high and low diffusivity and estimating diffusivity at an offset distance (Visser, 1997). With the additional term and offset, the random displacement model accounts for both uniform and non-uniform diffusivity. In a scenario with uniform diffusivity, the random displacement model equals the random walk model which makes the model a more viable choice than the limiting random walk model. Visser (1997) proved the need for the random displacement model when attempting to use random walk with non-uniform diffusivity, particles accumulated in low diffusivity regions which causes a non-physical, inverse diffusion.

For a 1-dimensional process, diffusivity, D_z, is relative to displacement, z, and time, t by $\frac{d}{dt}\left\langle z^2 \right\rangle = 2D_z$ (Taylor, 1921; Csanady, 1973; Holloway, 1994). Visser (1997) shows this relationship for an individual particle for a certain change in position which is expressed in an Euler method solution to this ODE as,

$$z_{n+1} = z_n + R\sqrt{2D_z \Delta t / r} \tag{3.1}$$

where R represents a random process, we used a random, normal distribution with a mean of 0, r is the standard deviation of the random process, in our case this was equal to 1, Δt is a finite time step, and n is the index to the time integration.

Due to the non-uniformity in marine environments, a simple random walk application gives inconsistent results. Much deliberation occurred over a resolution for these results with respect to the probability of the spatially varying diffusivity field which became a well-documented subject (J. Thomson, 1984; Okubo, 1986; Hunter et al., 1993; Visser, 1997). Shown by Visser (1997), a corrected random walk model or more commonly known as a random displacement model can be expressed as,

$$z_{n+1} = z_n + \frac{\partial D_{z_n}}{\partial z}\Delta t + R\sqrt{2D_{z_n + 0.5\frac{\partial D_{z_n}}{\partial z}\Delta t}\Delta t / r} \tag{3.2}$$

where there is an additional advective component defined by the diffusivity gradient and time step, and the diffusivity is now calculated offset a distance from the initial location. When the diffusivity gradient becomes uniform, or zero, the random displacement model becomes the random walk model again (Visser, 1997).

3.3.1 Vertical Diffusion

Vertical diffusivities are defined as a function of density, the Brunt Väisälä frequency, the Richardson number, and the dissipation rate of kinetic energy and can be used in modeling both in the mixed layer and beneath of the water column (Canuto et al., 2002). In mixed layer mixing, wind is considered the dominant force and is factored in the dissipation rate of kinetic energy, which is dependent on location. The dissipation becomes difficult to define given locations with varying topographies. Turbulence-scheme models are commonly used to estimate a diffusivity profile by Reynolds equations (Burchard and Baumert, 1995).

A general relationship between vertical and horizontal diffusivities is that the horizontal turbulent diffusivity is approximately 1000 times the vertical (Young et al., 1982). This is because currents are primarily dominant on the horizontal plane. A commonly accepted horizontal diffusion coefficient near the sea surface is 1 m^2/s for horizontal currents between 0 and 0.15 m/s (Matsuzaki and Fujita, 2014).

3.3.2 Empirical Diffusion Relationships

Vertical diffusivity profiles are calculated most commonly and accurately by turbulence-closure schemes where diffusion rates are determined by the relationship of eddy viscosity, turbulent kinetic energy, buoyancy, and shear (Burchard and Baumert, 1995). A simpler method is to calculate diffusion coefficients with empirical solutions such as the ones computed in Koh and Fan (1970) and Broecker and Peng (1982). Koh and Fan (1970) define an empirical solution which defines vertical diffusivity for near surface coastal waters and Broecker and Peng (1982) provide a similar solution for deep lakes and oceans. In both experiments, an inverse relationship between diffusivity and vertical density gradient was found, implying a constant buoyancy flux. The respective

experimental results are shown in Figures 3.3 and 3.4.

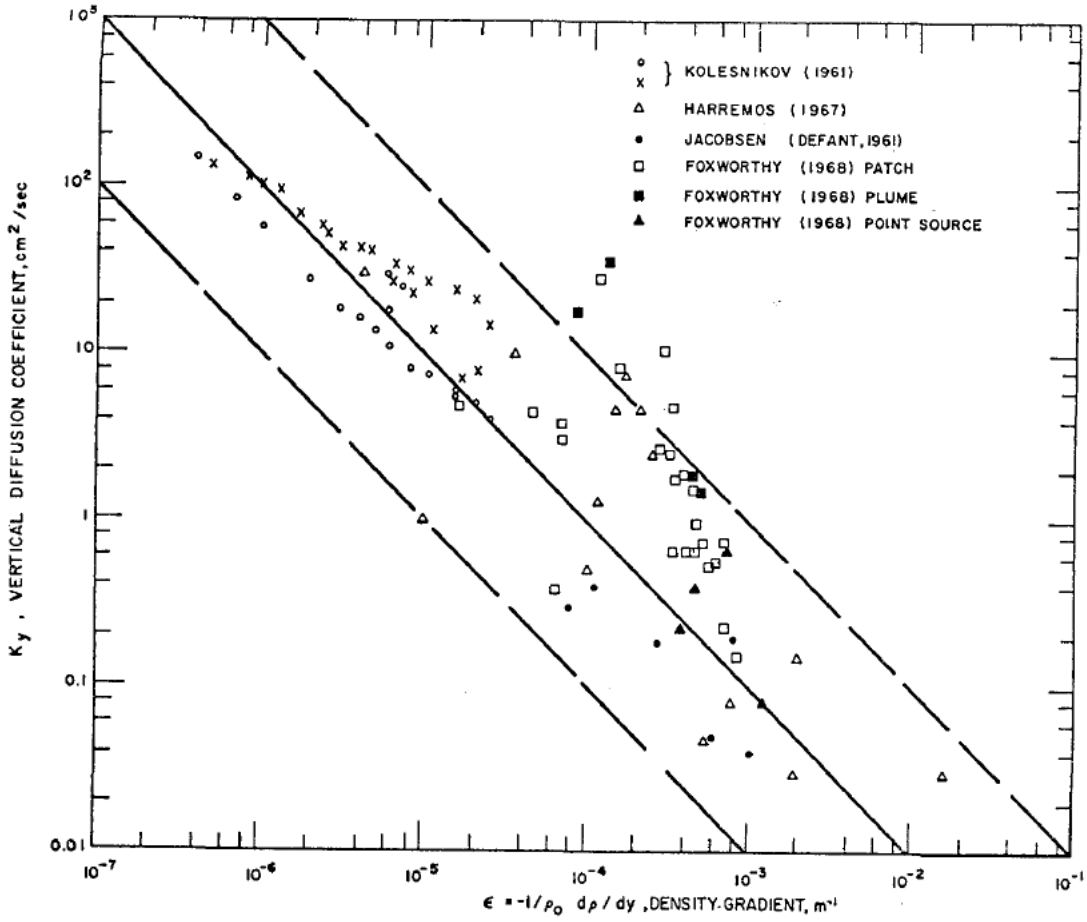

Figure 3.3: Inverse relationship between vertical diffusivity and density gradient reprinted from Koh and Fan (1970).

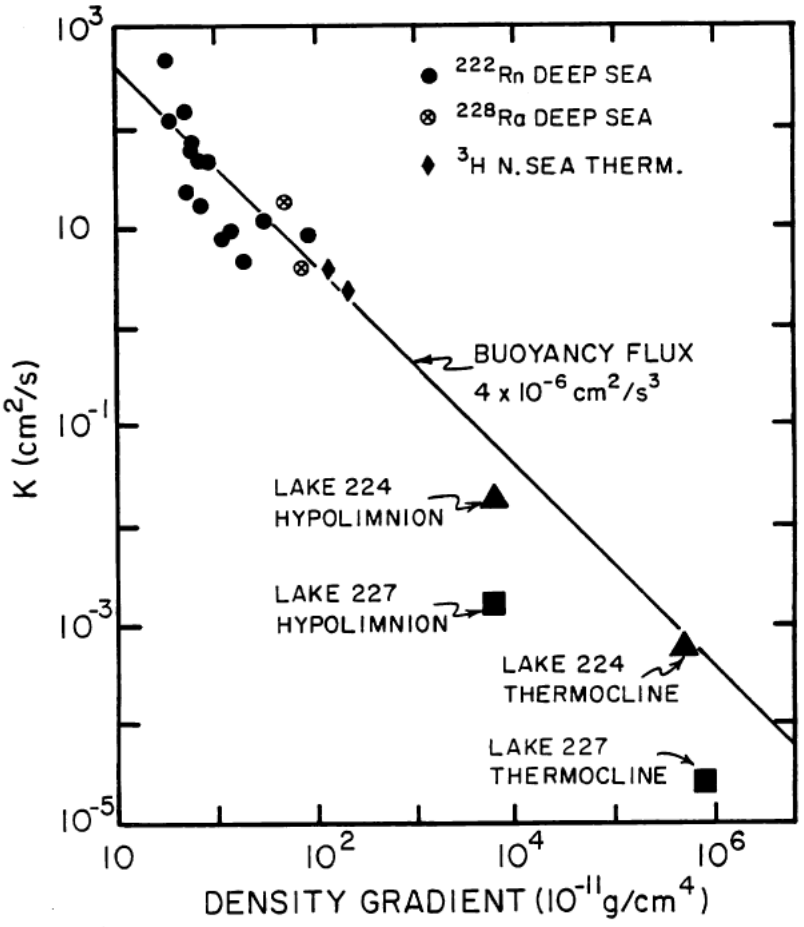

Figure 3.4: Inverse relationship between vertical diffusivity and density gradient reprinted from Broecker and Peng (1982).

Given the relationship shown in Figures 3.3 and 3.4, the empirical solutions are expressed by Koh and Fan (1970) and Broecker and Peng (1982) respectively as:

$$D_z = \frac{10^{-6}}{d\rho/dz} \tag{3.3}$$

$$D_z = \frac{4 \cdot 10^{-6}}{d\rho/dz} \tag{3.4}$$

where D_z is the vertical diffusivity in cm^2/s, ρ is the density of ambient seawater in g/cm^3, and z is the depth of the water column in cm. These models account for suppression of vertical diffusivity

by density stratification, but ignore the effects of currents and wind.

3.3.3 Diffusion Solution for Wind

Kullenberg (1971) provides an experimental solution for vertical diffusivity as a function of shear, stratification, and internal stress on the basis of the Reynolds stress formalism and backed by experimental data and previous research. Tracer measurements were recorded for stratified, shallow waters to determine vertical diffusion coefficient. Vertical diffusivity is a function of the density ratio, the Brunt Väisälä frequency, the Richardson number, and the dissipation rate of kinetic energy. Using the vertical diffusion function and experimental data Kullenberg (1971) found an empirical relationship between vertical diffusivity and the parameter, $(W^2/N^{-2})\,|dqdz|$ existed and expressed as,

$$D_z = constant \cdot \left(W^2\right)\left(N^{-2}\right)\frac{dq}{dz} \tag{3.5}$$

where W is wind velocity at a 10 meter elevation, N is the stratification frequency, and dq/dz is the vertical gradient of the horizontal current velocity of the water column i.e. the shear. This solution was derived from the relationship between energy supplied per unit time and volume by the shear stress, τ, Equation 3.6, and the relationship between wind stress, τ_0, drag coefficient, density, and wind speed, Equation 3.7,

$$-\frac{d}{dz}\left(q\tau\right) = -\tau\frac{dq}{dz} \tag{3.6}$$

$$\tau_0 = c_d \cdot \rho_a \cdot W^2 \tag{3.7}$$

assuming τ is constant and equal to τ_0 due to the assumption of a shallow water column. Kullenberg (1971) used these relationships to compute an empirical solution for vertical diffusion. The relationship found is expressed as,

$$D_z = -R_f C_d \frac{\rho_a}{\rho} \left(W^2\right) \left(N^{-2}\right) \frac{dq}{dz} \tag{3.8}$$

where R_f is the flux Richardson number, C_d is the drag coefficient, ρ is the density, and a is atmospheric. The flux Richardson number is defined as the ratio of the buoyancy of the turbulent kinetic energy and the energy consumed by work or shear terms. A mean value of experimental data was used for the flux Richardson number (0.05), and common estimates for shallow regions for drag coefficient $(0.95 \cdot 10^{-3} - 1.5 \cdot 10^{-3})$ and density ratio $(1.2 \cdot 10^{-}3)$ were assumed (Kullenberg, 1971). Kullenberg (1971) utilized the complete set of experimental results and the common assumptions aforementioned to derive the following empirical relationship for vertical diffusion and wind,

$$D_z = \left(8.9 \cdot 10^{-8}\right) \left(W^2\right) \left(N^{-2}\right) \left|\frac{dq}{dz}\right| \tag{3.9}$$

The empirical relationship derived in Kullenberg (1971) is shown in Figure 3.5.

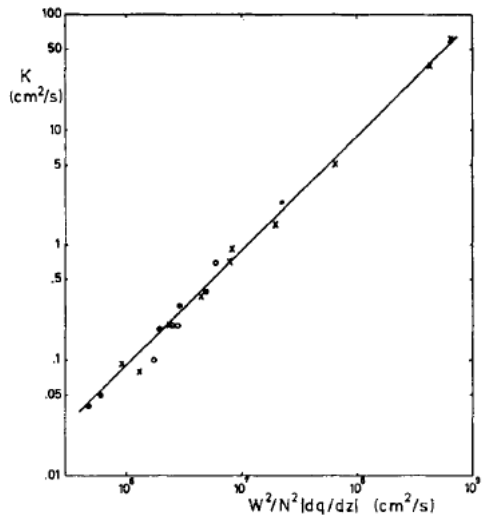

Figure 3.5: Linear relationship between vertical diffusivity and wind, buoyancy frequency, and shear reprinted from Kullenberg (1971).

3.4 Mixed Layer Depth

Surface winds affect the entire water column in shallow waters and the upper mixing layer in deeper waters (Sinha and Golshan, 2018). Mixed layer depth is most accurately defined by seawater and wave characteristics, a broad assumption used to estimate a mixed layer depth is commonly known as the threshold method. There are variations to the threshold method, the solution used in this thesis is one defined by Schneider and Müller (1990). A best approximate value of the mixed layer depth has been tested with experimental data and estimated as the vertical coordinate where there is more than a 0.01 kg/m^3 difference in potential density from the surface density. Measurements of the density at the surface tend to be unreliable, so the surface values are evaluated at approximately 2.5 m in depth (Schneider and Müller, 1990; Thomson and Fine, 2003). This threshold method is illustrated in Figure 3.6.

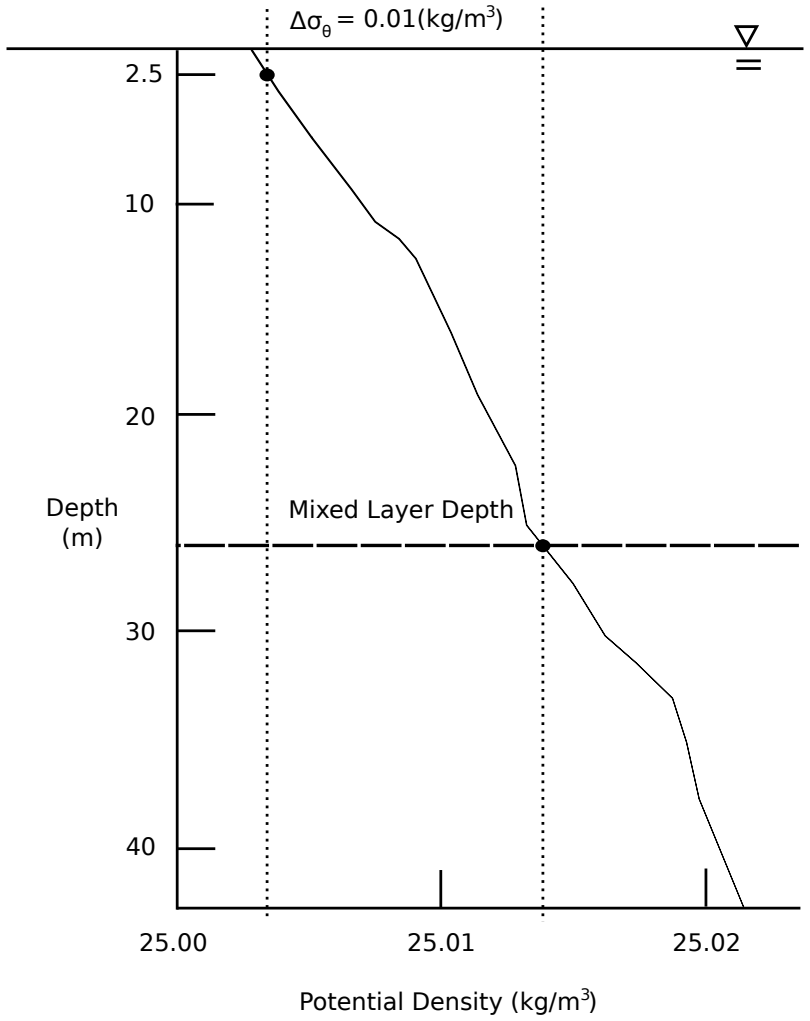

Figure 3.6: Mixed Layer Depth as defined by Schneider and Müller (1990).

3.5 Arctic Domain Awareness Center Scenarios

The Arctic Domain Awareness Center (ADAC) is supported by the Department of Homeland Security and hosted by the University of Alaska. ADAC's mission is to improve the ever changing Arctic environment through technology and education. ADAC supports the U.S. Coast Guard in it's search and rescue, humanitarian, disaster response, and security missions proving it's importance and remaining the only of its kind. ADAC has funded Texas A&M University to adapt TAMOC to better simulate Arctic conditions, including spills in shallow water and the effects of ice. Through this work, scenarios have been generated in TAMOC that represent possible Arctic spills. The

three scenarios along Alaska's coasts, used in this research and defined in Gros and Socolofsky (2017), consist of a tanker spill off Barrow, a pipeline rupture North-West of Prudhoe Bay, and a Burger well blowout. The ADAC scenarios will be used in this thesis to compare output from TAMOC-GNOME coupling codes using different random walk models for the Lagrangian particle transport. The scenarios are further described in Table 3.1.

Table 3.1: ADAC Scenario Inputs

Input	Tanker Spill	Pipeline Rupture	Well Blowout
Release Depth (m)	45.7	14.9	45.7
Release Volume (barrels/day)	750,000	10,000	23,100
Release Duration (days)	1	2	2
GOR	0	0	450
Release Orifice Diameter (m)	5	0.254	0.5
Release Temperature (deg C)	-1.6	37.22	37.22

4. METHODOLOGY

4.1 Overview

TAMOC is a Lagrangian particle tracking model with a pure advective transport process applied in the SBM. Random walk and random displacement were added to the transport process and validated for idealized cases. The results of TAMOC are entered as input into GNOME and evaluated for certain spill scenarios. The modules in TAMOC are modified to accommodate diffusivity profiles and random displacement transport. The main structure of the TAMOC-GNOME coupling is shown in Figure 4.1.

4.2 Impact of Properties

A subsurface oil spill is defined in TAMOC as a fixed volume at which TAMOC describes the physical and chemical interactions in a nearfield domain for oil, gas, and water. In this study, TAMOC has the ability to define the nearfield domain by a circular area from the release location. Once the spill reaches the nearfield range, the spill is passed to GNOME where farfield motion is applied such as ocean currents, winds, and diffusion. The properties of the oil type vary from ship to well to pipeline and can alter the expected trajectory due to differences in densities and viscosities, as these properties change with time. The velocity profile for the water column impacts the advection and ultimate transport of the oil particles. Lastly, wind direction and speed can impact the transport and spreading of an oil spill once it reaches the upper mixed layer of the water column.

4.3 Impact of Diffusive Transport

Diffusion is relevant when turbulent eddies and vertical mixing exists in a water column. Diffusion applies the action of random motions to particles to better define the concentration results of the particles volume. Although advective transport is effective in moving the center of mass of a spill with the direction of environmental forces, the addition of diffusive transport computes a realistic effect for particle exposure to turbulent eddies. The application of diffusive transport has

become popular due to its simplicity and multiple applications (Visser, 1997).

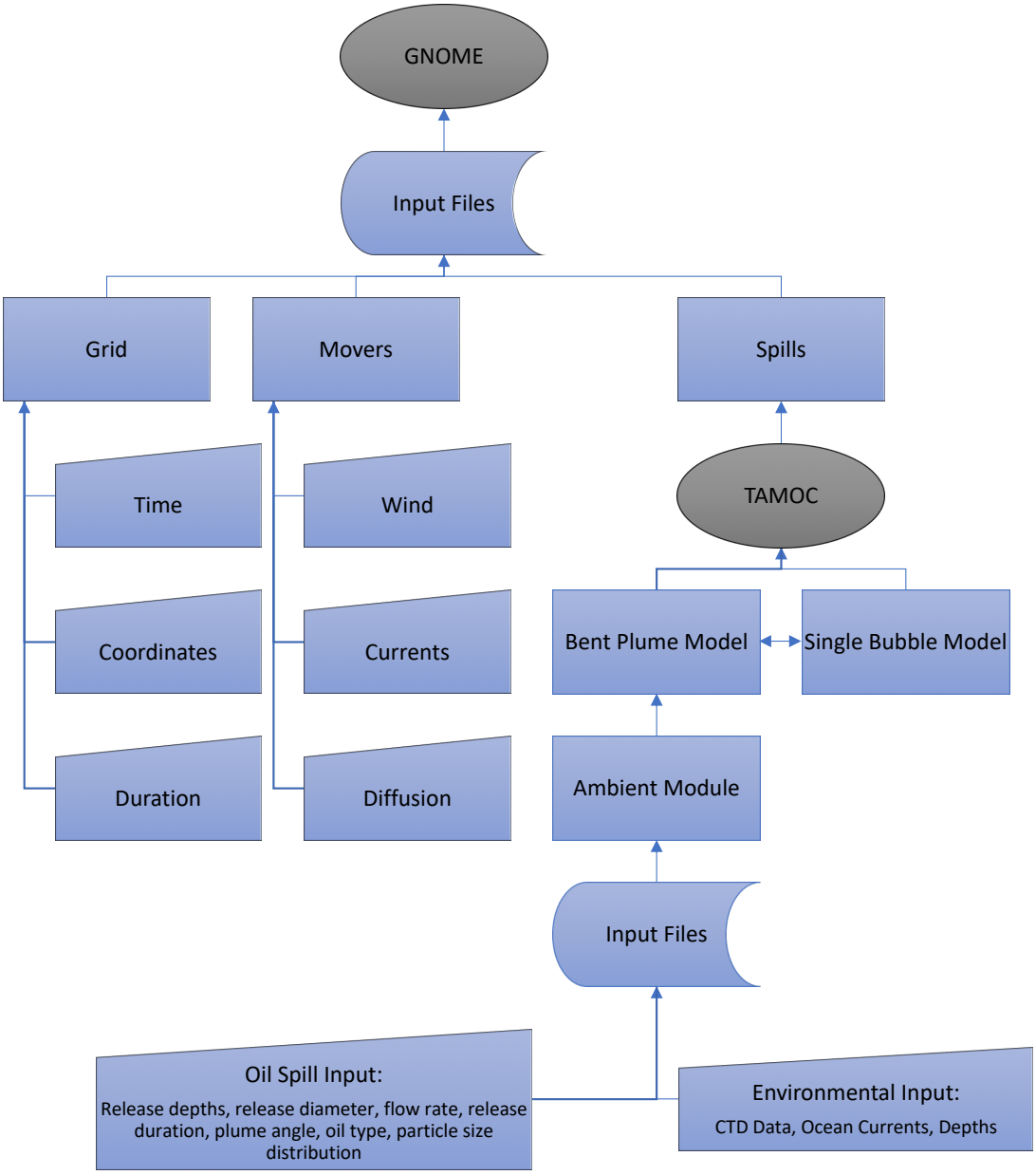

Figure 4.1: Main structure of TAMOC-GNOME coupling.

4.4 Environmental Input

TAMOC requires salinity and temperature profiles at the minimum for the ambient profile. The density for this data can then be computed and a depth profile can be further interpolated with correlating data using the ambient module. The ambient module is also capable of storing currents and diffusivities within the profile defined through the use of the profile-append function. The user is asked to input the environmental parameters which surround the spill in GNOME's "tamoc_spill.py" script and are shown in Table 4.1.

Table 4.1: "Tamoc_spill.py" Inputs for TAMOC - Environmental

Input	Description	Unit
depths	Vertical depth profile	m
nc_file	NetCDF4 profile	.nc
fname_ctd	CTD profile	.txt
ua	Velocity in x-direction	m/s
va	Velocity in y-direction	m/s
wa	Velocity in z-direction	m/s

GNOME also has environmental inputs for the coupling model. Within the simulation script, the user can define horizontal and vertical diffusion, currents, and winds which are all considered movers in GNOME. Table 4.2 describes the use of GNOME's movers.

Table 4.2: "Tamoc_script.py" Inputs for GNOME - Environmental

Parameter	Description	Input
model.movers + = PyCurrentMover	Circular current	current(m/s), method, extrapolate
model.movers + = SimpleMover	Current	x, y, z (m/s)
model.movers + = RandomVerticalMover	Diffusion	horizontal/vertical, above/below mixed layer, diffusion(cm^2/s)
model.movers + = constant_wind_mover	Wind	speed, direction, units

4.5 Oil Spill Input

TAMOC allows for the input of multiple parameters which describe a spill, this input is defined in the "tamoc_spill.py" script in GNOME. The more defined the spill is, the more accurate the model can predict the spill's transport and fate trajectory. The oil spill description parameters are listed in Table 4.3.

Table 4.3: "Tamoc_spill.py" Inputs for TAMOC - Oil Spill

Input	Description	Unit
release_time	Time spill intiated	datetime(year, month, day, hour, sec)
start_position	Initial location of spill	latitude, longitude, depth
end_release_time	Duration time of spill	start_time + timedelta(days)
diameter	Diameter of oil spill release orifice	m
release_temp	Temperature at spill release	K
release_phi	Vertical angle from horizontal of plume	$\pm\pi/2$
release_theta	Lateral angle in horizontal plane from x-axis to plume	$0 - 2\pi$ rad
release_flowrate	Spill flowrate at release	barrels per day
discharge_salinity	Salinity of continuous phase fluid	psu
tracer_concentration	passive tracer concentration	concentration
hydrate	Presence or absence of hydrates	boolean
dispersant	Presence or absence of dispersant	boolean
sigma_fac	Reduction in interfacial tension form dispersant	0 for gas, 1 for liquid
inert_drop	Liquid phase as inert	boolean
d50_gas	d_50 of gas particles	m
d50_oil	d_50 of oil particles	m
nbins	Number of particle size distribution bins	integer
fname_composition	Release fluid composition	.csv

The user can also apply weathering to the spill through the use of GNOME's weatherers pack-

age. There are many other combinations and applications but for the purposes of this study, we only utilize the weatherers as shown in Table 4.4.

Table 4.4: "Tamoc_script.py" Inputs for GNOME - Oil Spill

Parameter	Input
model.weatherers + = Evaporation	water, wind
model.weatherers + = Emulsification	water, wind, waves
model.weatherers + = NaturalDispersion	waves, water
model.weatherers + = Dissolution	waves

4.6 Procedure

4.6.1 Define Diffusivity

Canuto et al. (2002) defines a widely known method of using a Reynolds stress-based model to define vertical diffusivities as a function of density, the Brunt Väisälä frequency, the Richardson number, and the dissipation rate of kinetic energy. We needed a simpler application due to the lack of wave characteristics and eddy information. Therefore, we define diffusivity with empirical relationships found by Broecker and Peng (1982) for deep water scenarios, Koh and Fan (1970) for coastal and shallow waters, and Kullenberg (1971) for mixed layer depths with surface winds. Varying options for diffusivity profiles are now available in the model. Diffusivity can be defined by Broecker and Peng (1982)'s solution, Equation 3.4, which should be utilized for simulations in deeper depths. Diffusivity can also be defined by Koh and Fan (1970)'s solution, Equation 3.3, which is defined for shallower simulations. Kullenberg (1971)'s solution, Equation 3.6, is best applied in the upper mixed layer, the mixed layer depth is defined by the potential density threshold method. Equation 3.6 requires the current velocity shear, which is defined by a calculated mean from ADCP data collected from the Klondike, Burger, and Statoil Survey areas in the Chukchi Sea by the University of Alaska in 2010.

The profile-append function within the "tamoc_spill.py" file is used to store the empirical so-

lutions for defining diffusivity profiles with CTD and ambient data. The inputs needed to define diffusivity provided the use of the empirical solutions are displayed in Table 4.5. The user has the option to select the empirical relationship from the file in order to run different solutions and combinations of diffusion profiles.

Table 4.5: Define Diffusivity - Variables

Input	Description	Unit
z	Vertical depth profile	m
T	Temperature profile	K
S	Salinity profile	psu
P	Pressure profile	Pa
N	Buoyancy Frequency	1/s
W	Wind	m/s
dudz	Horizontal velocity shear	1/s
dz	Vertical step size	m

The CTD profile used in this study was defined in Gros and Socolofsky (2017) and based on regional field observations which represent environmental conditions during the end of the Arctic winter. The profile used in all test cases for this study is plotted in Figure 4.2.

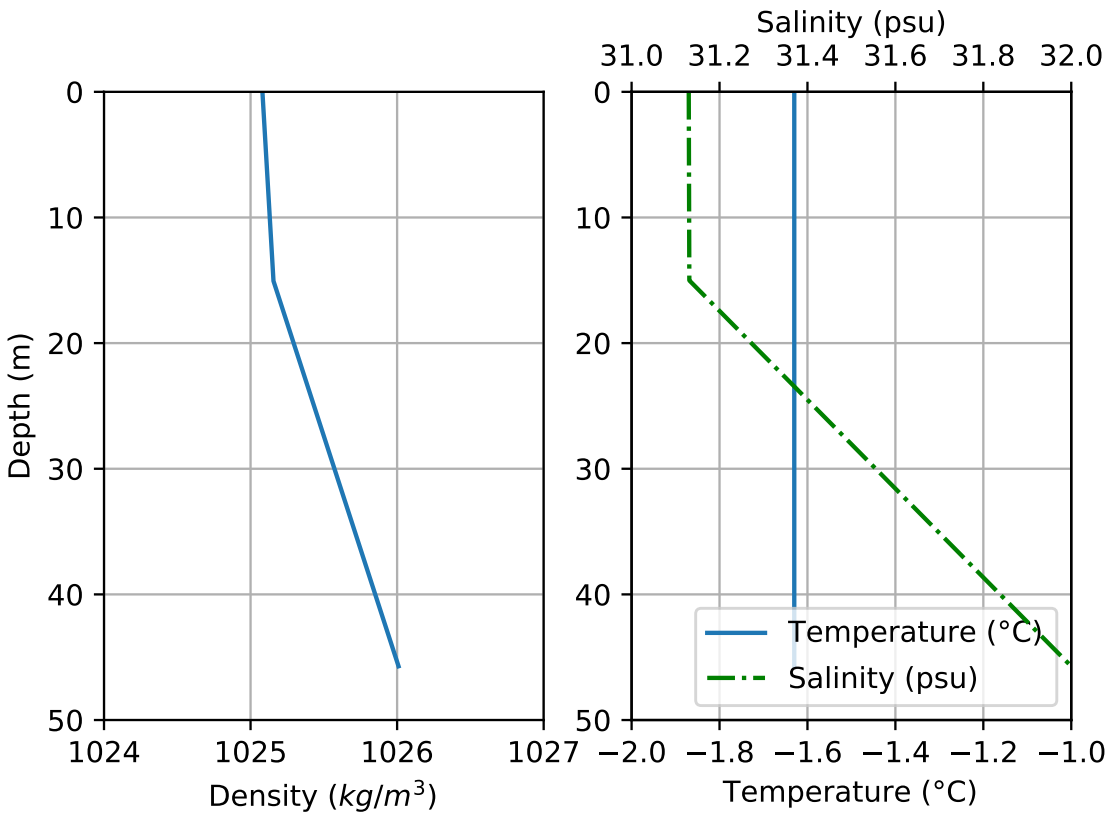

Figure 4.2: Alaska CTD Profile and computed density profile.

The diffusivity profiles were defined from the aforementioned CTD data set and computed pressure and densities. The diffusivity profiles are shown in Figure 4.3 and Figure 4.4. The Kullenberg (1971) solution for wind and diffusion is applied to an estimated upper mixed layer computed by the potential density threshold method defined by Schneider and Müller (1990). For random walk simulations, an averaged vertical diffusivity of 0.001 m^2/s from empirical solutions was used to define a constant diffusivity profile.

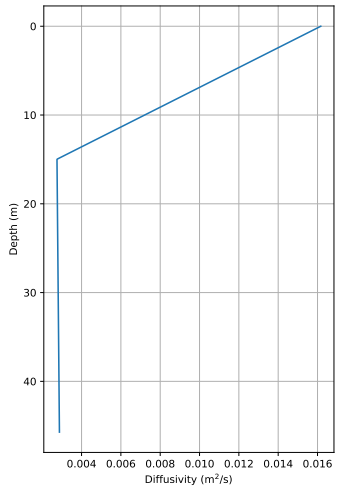

(a) Broecker and Peng (1982).

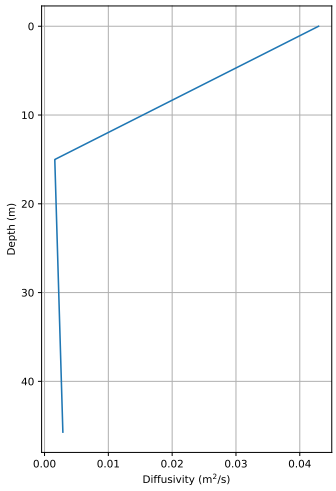

(b) Broecker and Peng (1982) and Kullenberg (1971), Wind = 5 m/s.

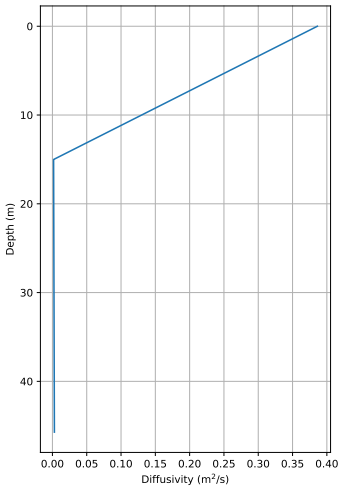

(c) Broecker and Peng (1982) and Kullenberg (1971), Wind = 15 m/s.

Figure 4.3: Diffusivity profiles defined by empirical solutions for diffusion.

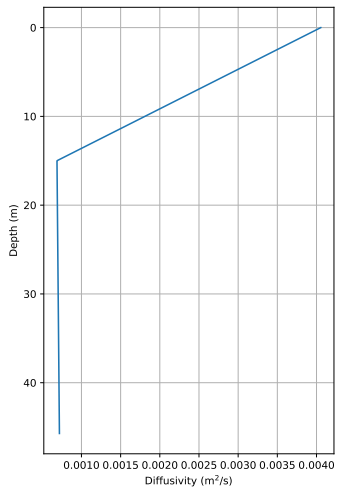

(a) Koh and Fan (1970).

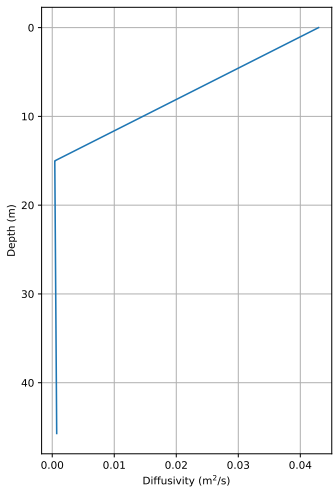

(b) Koh and Fan (1970) and Kullenberg (1971), Wind = 5 m/s.

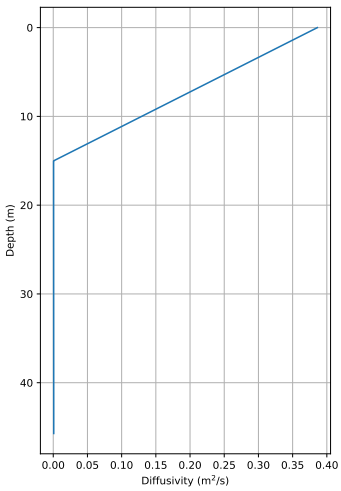

(c) Koh and Fan (1970) and Kullenberg (1971), Wind = 15 m/s.

Figure 4.4: Diffusivity profiles defined by empirical solutions for diffusion.

4.6.2 Single Bubble Model Modification

The SBM applies pure advection to each particle through ambient conditions and slip velocity. In this study, a random walk application and random displacement application were included using a fourth-order Runge-Kutta method to solve the set of ODEs. Random walk is the accepted method for horizontal diffusion due to the small effect and variance in the horizontal direction. We applied the random walk scheme to both the x- and y-directions and assumed a horizontal diffusivity of 0.01 m/s, this is a commonly accepted value for horizontal diffusivity. We manipulated the random walk and random displacement equations, Equation 3.1 and Equation 3.2, into a desired form needed to apply diffusive transport with the defined advection equations which is shown in Equation 4.1. The final equations for the vertical trajectory for random walk and random displacement are expressed in a Euler method solution for a particle tracking model in Equation 4.2 and Equation 4.3,

$$z_{n+1} = z_n + R\sqrt{2D_z\Delta t/r}$$

$$dz = R\sqrt{2D_z\Delta t/r}$$

$$\frac{dz^2}{dt^2} = \frac{R^2 2D_z\Delta t/r}{dt^2}$$

$$\frac{dz}{dt} = R\sqrt{2D_z/\Delta t \cdot r}, r = 1 \tag{4.1}$$

$$\frac{dz}{dt} = -u_s - w_a + R\sqrt{2D_z/\Delta t} \tag{4.2}$$

$$\frac{dz}{dt} = -u_s - w_a - \frac{dD_z}{dz} + R\sqrt{2D_z/\Delta t} \tag{4.3}$$

where $\frac{dz}{dt}(m/s)$ is the vertical velocity, $u_s(m/s)$ is the slip velocity, $w_a(m/s)$ is the vertical current, $\frac{dD_z}{dz}(m/s)$ is the diffusivity gradient with respect to a user-defined step size, R is a random number between 0 and 1, D_z is the vertical diffusivity (m^2/s), and $\Delta t(s)$ is a user-defined time step.

Visser (1997) discusses the importance of determining the proper method when modeling a trajectory and proved the inaccuracy of random walk with non-uniform diffusivity, by showing non-buoyant, uniformly distributed particles accumulating in low diffusivity regions which causes a non-physical, inverse diffusion. We replicated Visser (1997)'s experiment and validated TAMOC's defined diffusivity and random displacement application by receiving the same results. Figure 4.5 demonstrates the Random Walk application to a non-uniform diffusivity profile in 4.5a, there is visible variation where particles are no longer uniformly spaced due to low diffusivity regions at approximately z = 10 m. Figure 4.5b shows a much better distribution of particles similar to where they started vertically. The experiment was identical to Visser (1997) in calculating the trajectory of 4000 particles, for 6 hours over 10 minute intervals for a depth of 40 meters.

We also analyzed a single droplet trajectory to ensure randomness occurred in all directions when applying the random walk and random displacement schemes. We assumed particles that reached the surface resuspended randomly through the upper mixed layer and applied that to the SBM which can be seen in the following figures. The resuspension of particles was applied to simulate the vertical mixing caused by the breaking of waves by reflecting the particles randomly through the upper ocean layer once surfaced. The results were as expected with varying outputs each time the model ran. Figure 4.6 displays the previous output from a pure advective transport model, there is no variation and a straight trajectory. Figures 4.7 and 4.8 display the output from random walk applied horizontally and random displacement applied vertically for diffusivity profiles defined by Koh and Fan (1970) and Broecker and Peng (1982), respectively with the second image containing the empirical relationship for wind and diffusion defined by Kullenberg (1971).

A maximum nearfield range is newly defined in the SBM in order to define when TAMOC

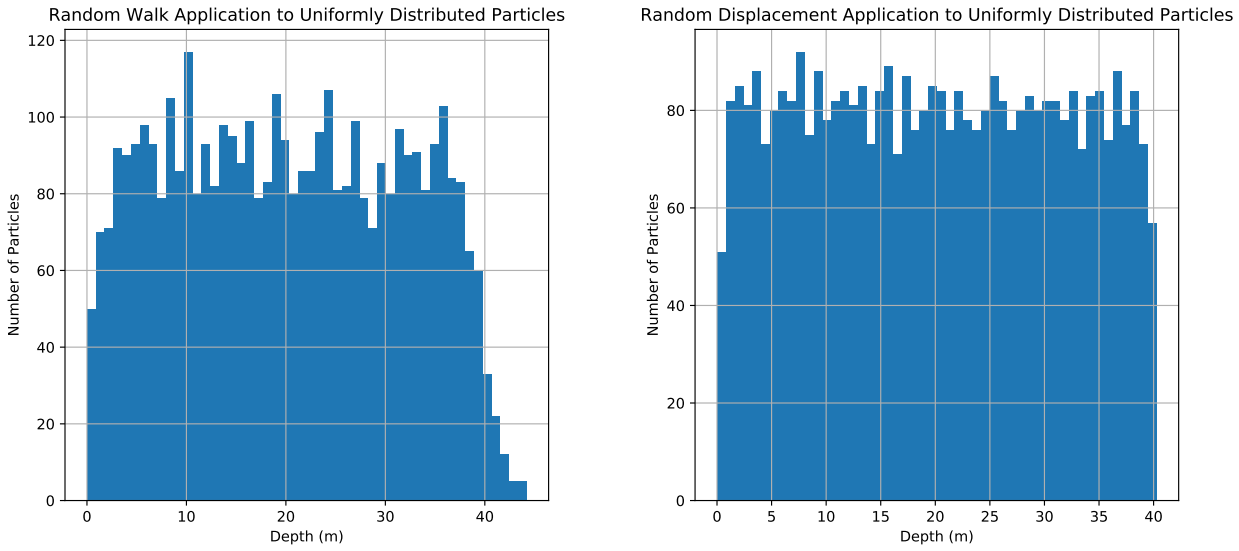

(a) (b)

Figure 4.5: Visser (1997) experiment recreated in TAMOC to validate correctness of random displacement over random walk for non-uniform diffusivity.

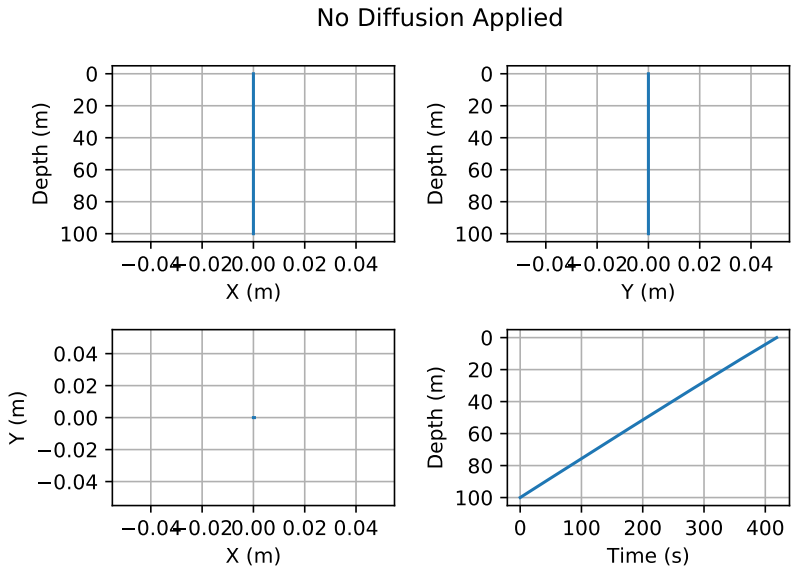

Figure 4.6: Single particle trajectory exposed to pure advective transport.

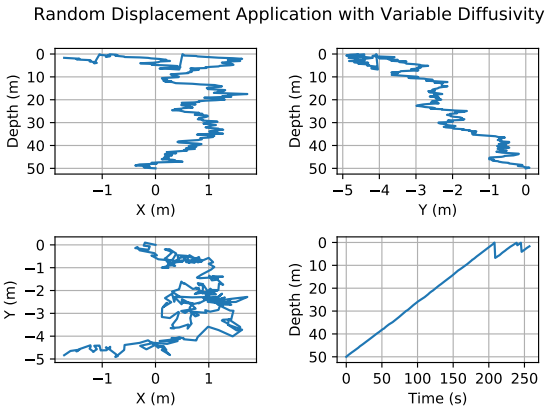

(a) Koh and Fan (1970)

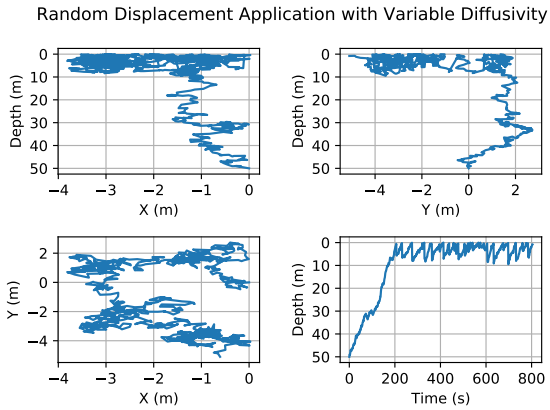

(b) Koh and Fan (1970) and Kullenberg (1971)

Figure 4.7: Single particle trajectory exposed to advective and diffusive transport (Koh and Fan, 1970; Kullenberg, 1971).

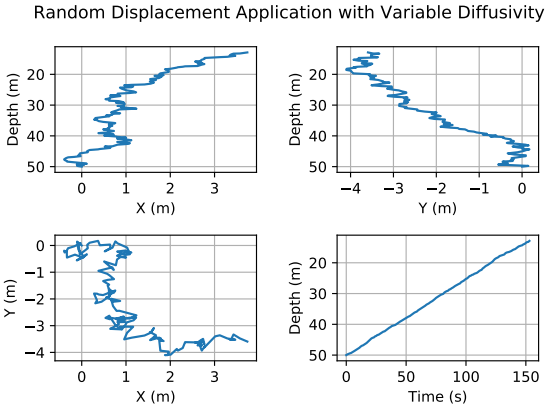

(a) Broecker and Peng (1982)

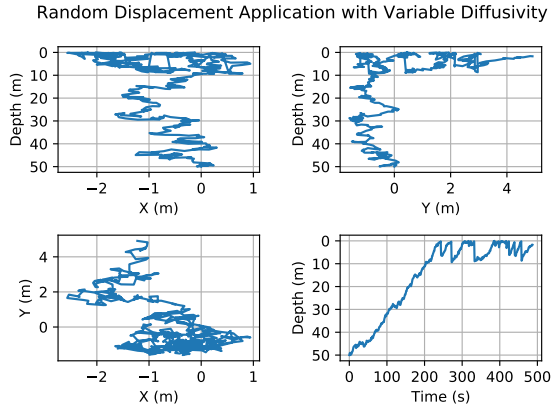

(b) Broecker and Peng (1982) and Kullenberg (1971)

Figure 4.8: Single particle trajectory exposed to advective and diffusive transport (Broecker and Peng, 1982; Kullenberg, 1971).

passes particles to GNOME. The proper range varies with oil properties and water depth, this is modified in the "RK4_solver" function defined in the SBM. The range becomes a limiting factor when running the TAMOC-GNOME coupled model, the default value is 10 km but can be altered.

4.6.3 Bent Plume Model Modification

The BPM was modified to track all particles inside and outside the plume in order to send all particle location to GNOME once they have reached the end of the nearfield domain or range defined in the SBM. The input "t_max" is also modified in the BPM in order to add another limit in case the range defined is too far. The default value is 100,000 seconds but can be altered.

4.7 TAMOC-GNOME Coupling

It is a great asset to have the benefits of both TAMOC and GNOME in an oil spill simulation. TAMOC utilizes a deep-water plume model and features deep-water chemistry analysis and GNOME includes a larger spatial scale and includes sea surface and weathering processes. The deep-water plume analysis will be sent to GNOME once transport processes finish and particles reach the end of buoyant effects. GNOME can then analyze the spill scenario at the sea surface for weathering processes and trajectory. This is all completed in one script which defined all inputs for GNOME and TAMOC and a spill scenario and is run in Python.

The same data was used for all spill scenarios in both TAMOC and GNOME. A mixed layer depth of 15 meters was used in all scenarios.

5.1 Script Tamoc

GNOME's installed package supplies a sample oil spill and script to couple TAMOC and GNOME. After modifying the TAMOC modules and "tamoc_spill.py" file in GNOME, we first tested random diffusion in TAMOC with the example script. The example script has the following TAMOC spill parameters:

Table 5.1: "Tamoc_script.py" Inputs for TAMOC - Oil Spill

Parameter	Input
release_time	datetime(2004, 12, 31, 13, 0)
start_position	(0, 0, 300)
end_release_time	start_time + timedelta(days=3)
diameter	0.3 m
release_temp	423.15 K
release_phi	$-\pi/2$
release_theta	0 rad
release_flowrate	20,000 barrels per day
discharge_salinity	0 psu
tracer_concentration	1
hydrate	True
dispersant	False
sigma_fac	np.array([[1.], [1. / 200.]])
inert_drop	False
d50_gas	0.008 m
d50_oil	0.0038 m
nbins	20

In addition to the TAMOC parameters, currents and diffusion were applied on the GNOME

farfield calculation. A 0.3 m/s southern circular current and a 0.1 m/s eastward current were applied in addition to a 0.05 m/s vertical diffusivity above the mixed layer and a 0.0011 m/s vertical diffusivity below the mixed layer depth were applied using the random walk method in GNOME.

We tested TAMOC first to ensure the model was applying random walk (RW) and random displacement (RD) as expected. The differences in vertical location between pure advection, random walk, and random displacement applications are displayed in Figure 5.1 and Figure 5.2. These figures show the differences in vertical locations at the end of the near field domain in TAMOC. The random displacement histograms show more variability with depth versus pure advection, with Koh and Fan (1970)'s solution having remaining particles in the upper 25 meters and Broecker and Peng (1982)'s solution having remaining particles in the upper 100 meters. Broecker and Peng (1982)'s solution is more suited for this scenario with a deep water colum of $300m$.

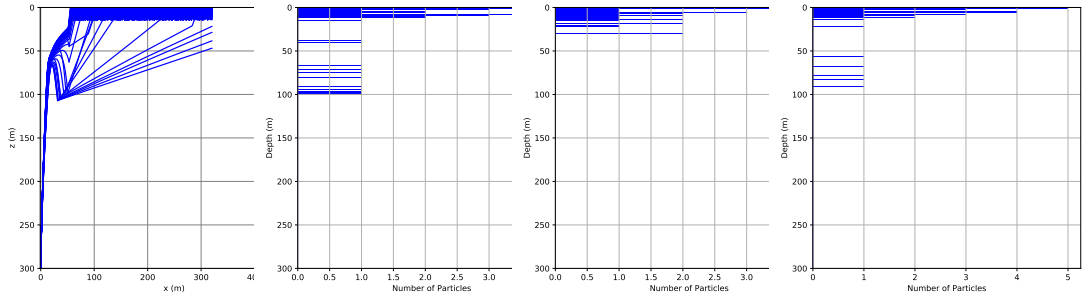

(a) TAMOC Advection Plume (b) Random Walk (c) RD(Koh and Fan, 1970) (d) RD(Broecker and Peng, 1982)

Figure 5.1: Script - TAMOC Results

In Figure 5.2, all graphs are displaying random displacement. Figure 5.2 (a) and (b) are generated with Koh and Fan (1970)'s solution and Kullenberg (1971)'s applied to the mixed layer, and (c) and (d) are generated with Broecker and Peng (1982)'s solution and Kullenberg (1971)'s applied to the mixed layer.

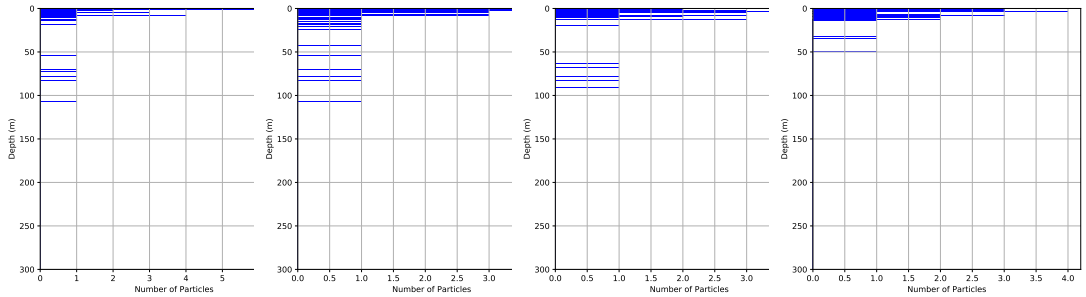

(a) 5 m/s Wind (b) 15 m/s Wind (c) 5 m/s Wind (d) 15 m/s Wind

Figure 5.2: Script - TAMOC Results with Wind

We coupled TAMOC with GNOME to compute a farfield trajectory. These results for Script are shown in the following figures:

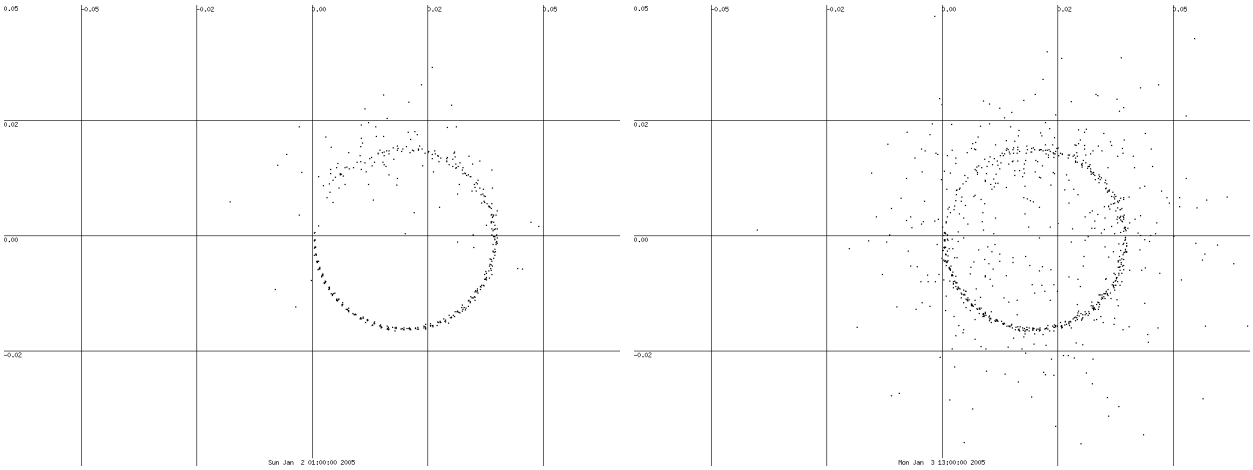

(a) Elapsed time: 1 day (b) Elapsed time: 2 days

Figure 5.3: Script - Pure Advection

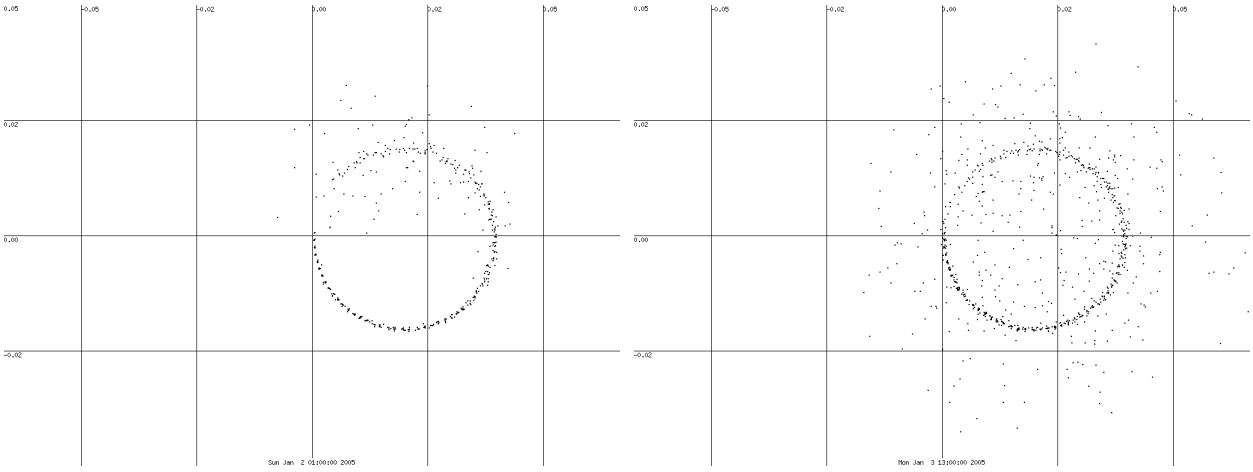

(a) Elapsed time: 1 day (b) Elapsed time: 2 days

Figure 5.4: Script - Random Walk

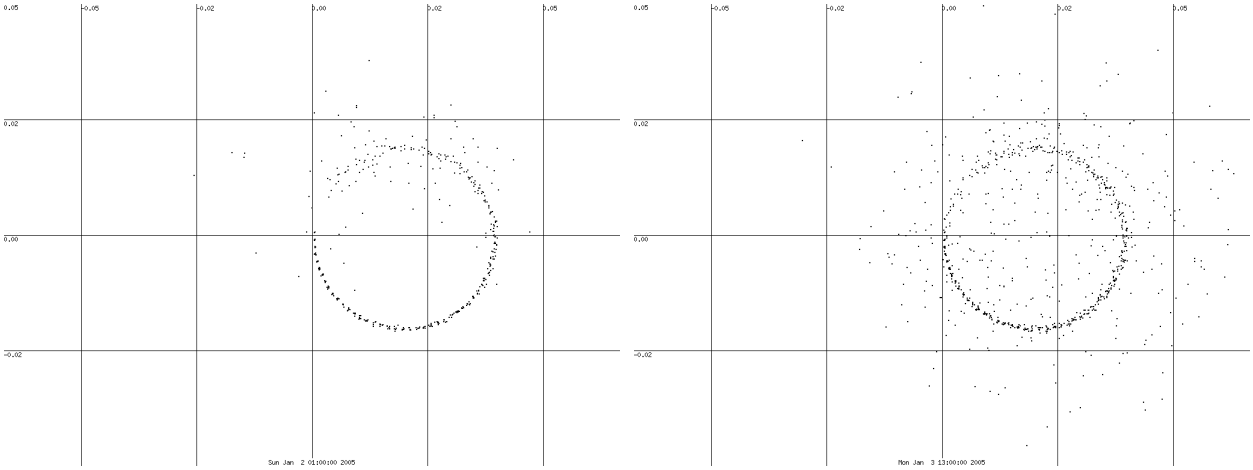

(a) Elapsed time: 1 day (b) Elapsed time: 2 days

Figure 5.5: Script - Random Displacement (Koh and Fan, 1970)

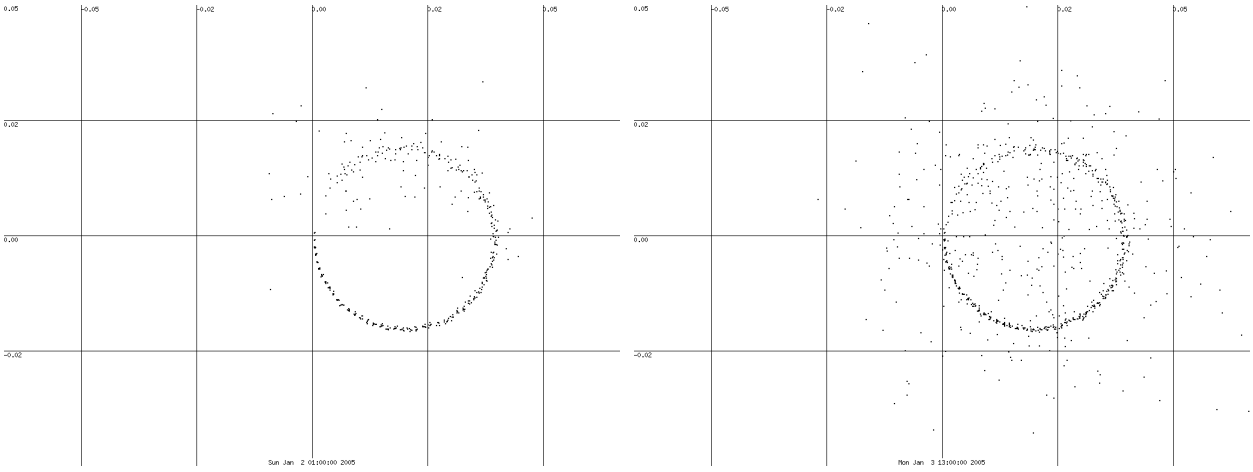

(a) Elapsed time: 1 day (b) Elapsed time: 2 days

Figure 5.6: Script - Random Displacement (Broecker and Peng, 1982)

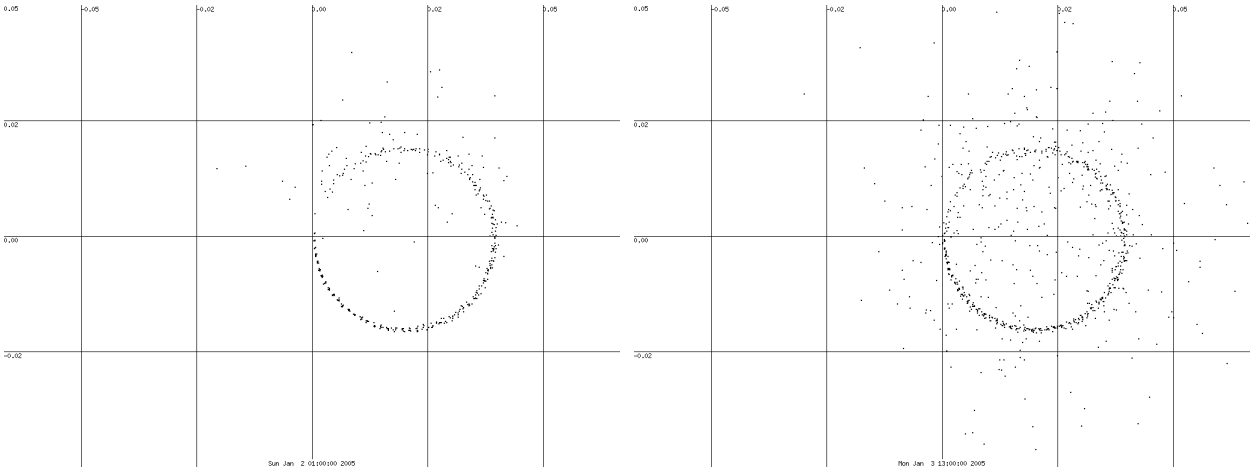

(a) Elapsed time: 1 day, Wind = 5 m/s (b) Elapsed time: 2 days, Wind = 5 m/s

Figure 5.7: Script - Random Displacement (Broecker and Peng, 1982; Kullenberg, 1971)

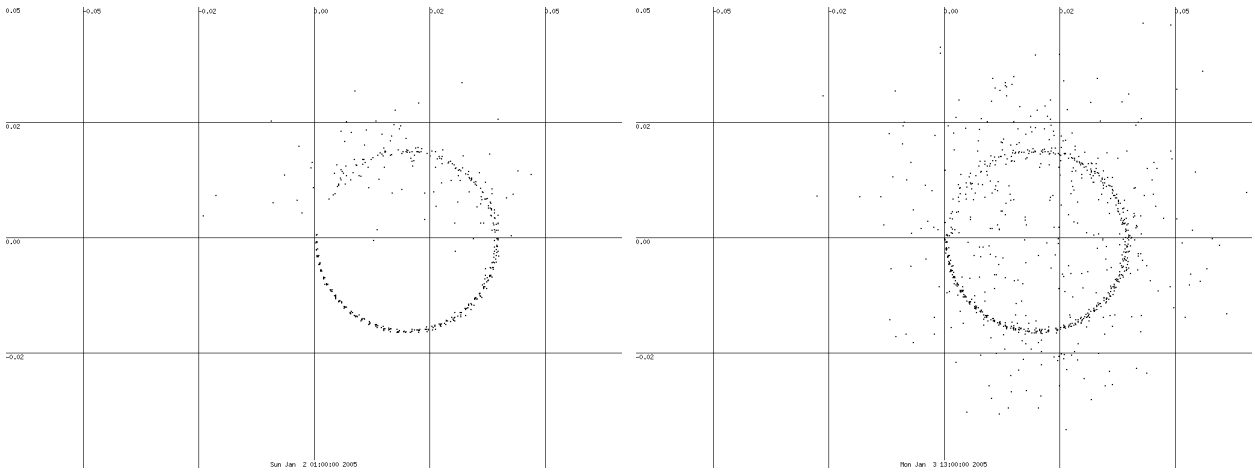

(a) Elapsed time: 1 day, Wind = 5 m/s (b) Elapsed time: 2 days, Wind = 5 m/s

Figure 5.8: Script - Random Displacement (Koh and Fan, 1970; Kullenberg, 1971)

The GNOME output from Script demonstrate the existence of the circular current applied in GNOME, but still show the effects of added diffusion to an oil trajectory. Due to the circular currents applied, pure advection does a decent job of predicting the oil spill fate, Figure 5.3. In Figure 5.4, the particles are concentrated within the center of mass for the spill, this is because there is more vertical mixing present with the addition of a random walk scheme. The best plot for this scenario is Figure 5.8. In this plot, Kullenberg (1971)'s solution is dominant and computes a higher vertical diffusivity due to wind forcing and a shallow water column.This plot shows random movement and less of a concentration of particles at the release location, this is an expected result.

5.2 ADAC Scenario 1: Tanker Spill off Barrow

In this scenario, an oil tanker has an accident, sinks, and releases cargo from the seafloor. ADAC Scenario 1 has the following TAMOC spill parameters:

Table 5.2: "Scenario1.py" Inputs for TAMOC - Oil Spill

Parameter	Input
release_time	datetime(2016, 05, 04, 13, 0)
start_position	(-156.8, 71.5, 45.7)
end_release_time	start_time + timedelta(days=2)
diameter	5.0 m
release_temp	271.55 K
release_phi	$-\pi/2$
release_theta	0 rad
release_flowrate	750,000 barrels per day
discharge_salinity	0 psu
tracer_concentration	1
hydrate	True
dispersant	False
sigma_fac	np.array([[1.], [1. / 200.]])
inert_drop	False
d50_gas	0.008 m
d50_oil	0.0038 m
nbins	20

The TAMOC results for comparing the differences in vertical location between pure advection, random walk, and random displacement applications are displayed in Figure 5.9 and Figure 5.10. These figures show the differences in vertical locations at the end of the near field domain in TAMOC. The random displacement histograms show much more variability with depth, where both solutions show particle distribution throughout the water column. Koh and Fan (1970)'s

solutions has the best results of a well-mixed profile. The particles much deeper in the water column are caused by stopping the model simulation before the full spill has reached the upper ocean layer. There are no currents in this scenario so the spill moves much slower.

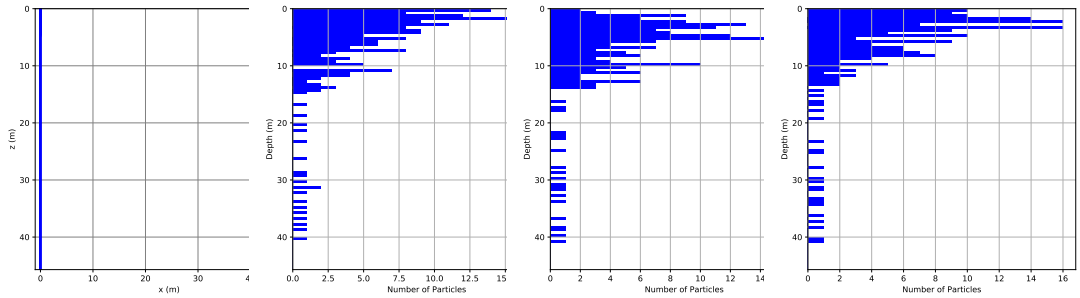

(a) TAMOC Advection Plume (b) Random Walk (c) RD(Koh and Fan, 1970) (d) RD(Broecker and Peng, 1982)

Figure 5.9: ADAC Scenario 1 - TAMOC Results

In Figure 5.10, both graphs are displaying random displacement. Kullenberg (1971)'s solution assumes the entire depth of the water column due to the shallow depth. The oil particles are approximately, evenly distributed among the entire water column representing the effect of wind forcing in a shallow water. The solution for a wind speed of $15m/s$ has much greater vertical distribution, where particles still remain closer to the surface with a $5m/s$ wind.

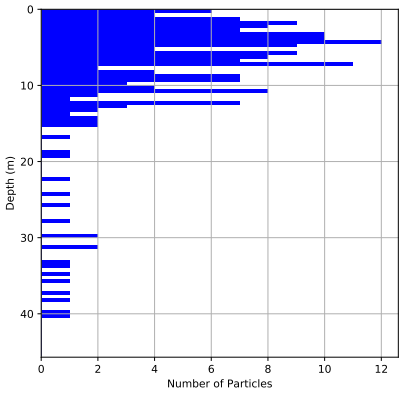

(a) 5 m/s Wind

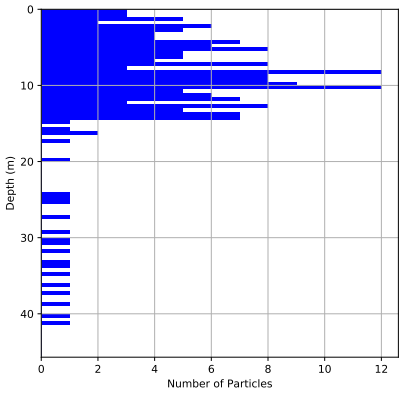

(b) 15 m/s Wind

Figure 5.10: ADAC Scenario 1 - TAMOC Results with Wind

The coupled results from TAMOC and GNOME for a farfield trajectory for Scenario 1 are shown in the following figures:

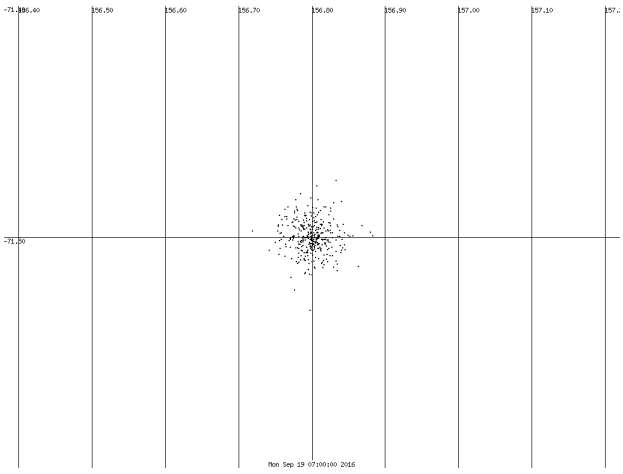

(a) Elapsed time: 0.5 day

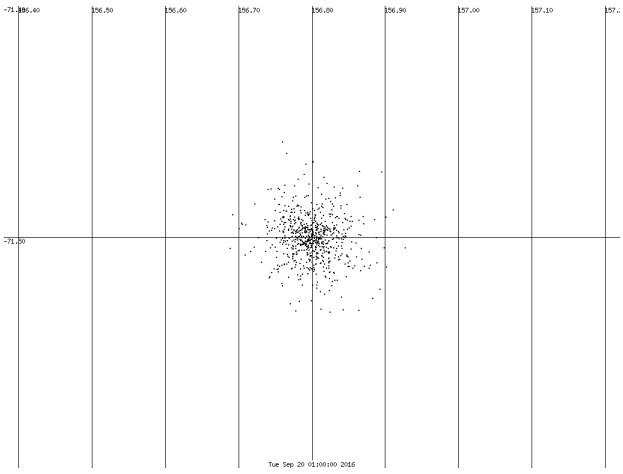

(b) Elapsed time: 1 day

Figure 5.11: Scenario 1 - Pure Advection

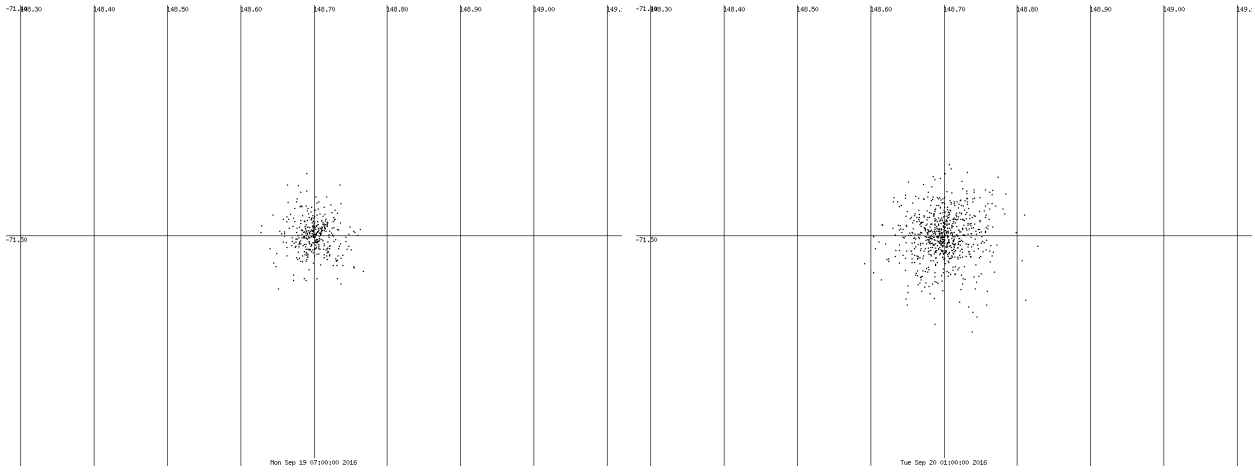

(a) Elapsed time: 0.5 day (b) Elapsed time: 1 day

Figure 5.12: Scenario 1 - Random Walk

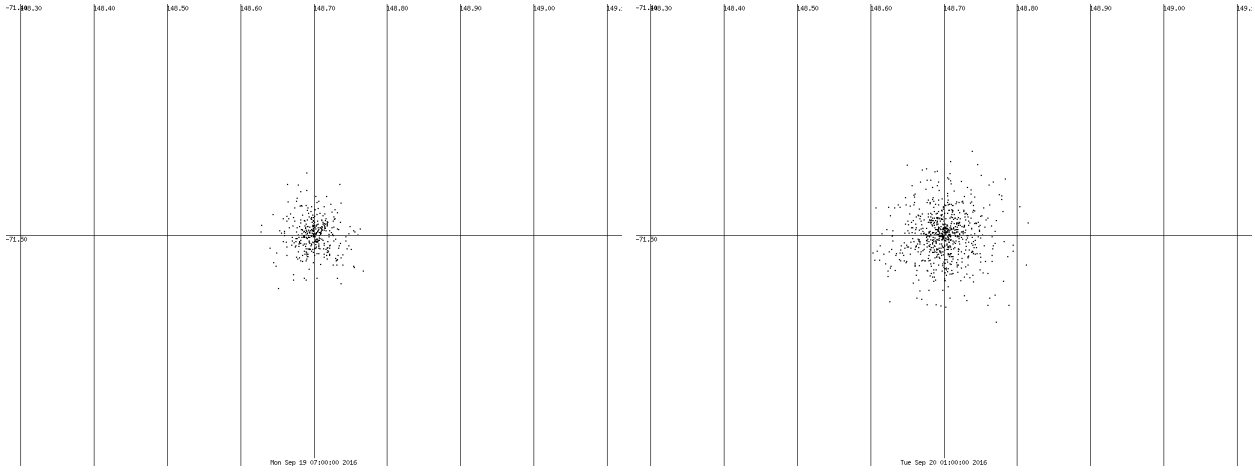

(a) Elapsed time: 0.5 day (b) Elapsed time: 1 day

Figure 5.13: Scenario 1 - Random Displacement (Koh and Fan, 1970)

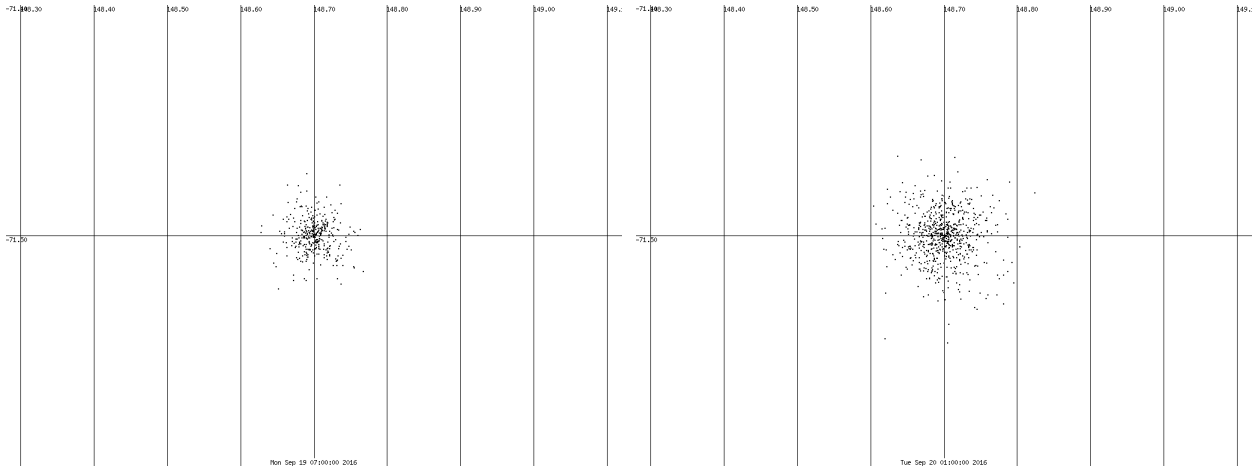

(a) Elapsed time: 0.5 day (b) Elapsed time: 1 day

Figure 5.14: Scenario 1 - Random Displacement (Broecker and Peng, 1982)

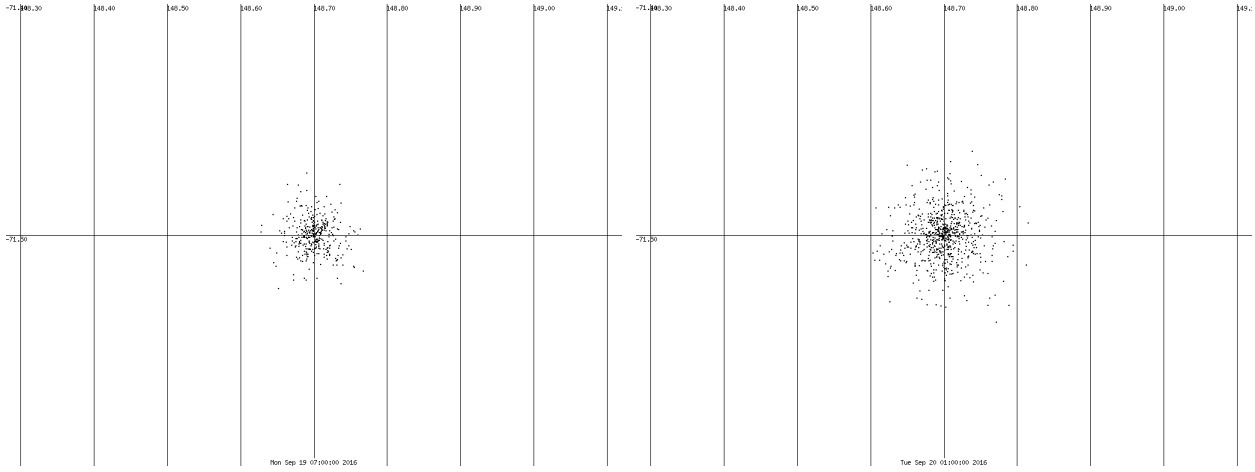

(a) Elapsed time: 0.5 day, Wind = 5 m/s (b) Elapsed time: 1 day, Wind = 5 m/s

Figure 5.15: Scenario 1 - Random Displacement (Broecker and Peng, 1982; Kullenberg, 1971)

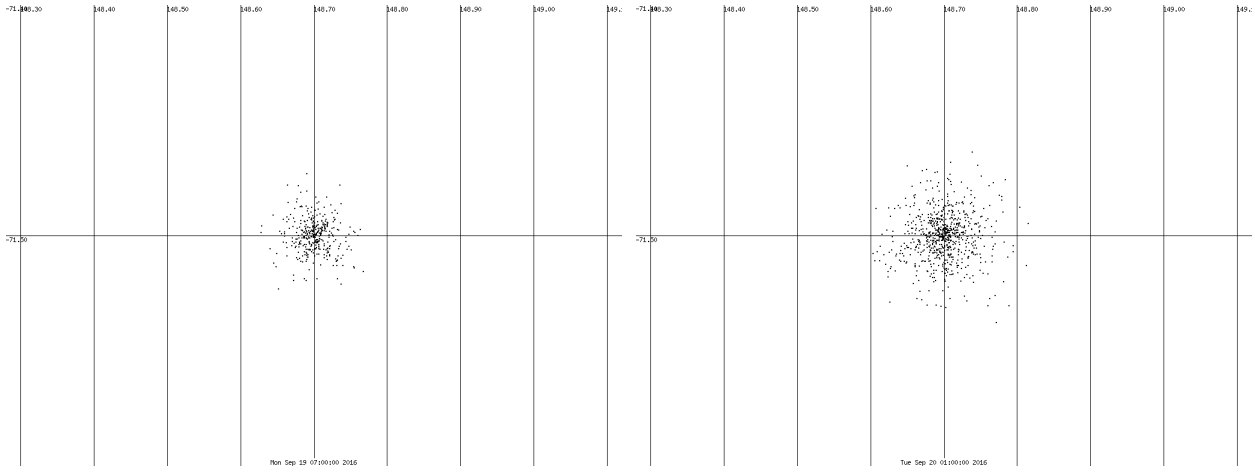

(a) Elapsed time: 0.5 day, Wind = 5 m/s (b) Elapsed time: 1 day, Wind = 5 m/s

Figure 5.16: Scenario 1 - Random Displacement (Koh and Fan, 1970; Kullenberg, 1971)

The GNOME output from Scenario 1 shows the effects of added diffusion to an oil trajectory. This scenario is only for the duration of one day, so results do not vary by a large amount. The difference is still noticeable when comparing Figure 5.12, where Random Walk was applied, with the random displacement figures. In the random displacement plots, particles lie further from the center of the oil spill due to the random transport.

5.3 ADAC Scenario 2: Rupture of Northstar Island pipeline

ADAC Scenario 2 represents a situation where ice wore a pipeline to the point of severing and oil was released horizontally. ADAC Scenario 2 has the following TAMOC spill parameters:

Table 5.3: "Scenario2.py" Inputs for TAMOC - Oil Spill

Parameter	Input
release_time	datetime(2016, 05, 04, 13, 0)
start_position	(-156.8, 71.5, 14.9)
end_release_time	start_time + timedelta(days=2)
diameter	0.254 m
release_temp	310.37 K
release_phi	$-\pi/2$
release_theta	0 rad
release_flowrate	10,000 barrels per day
discharge_salinity	0 psu
tracer_concentration	1
hydrate	True
dispersant	False
sigma_fac	np.array([[1.], [1. / 200.]])
inert_drop	False
d50_gas	0.008 m
d50_oil	0.0038 m
nbins	20

The TAMOC results for comparing the differences in vertical location between pure advection, random walk, and random displacement applications are displayed in Figure 5.17 and Figure 5.18. These figures show the differences in vertical locations at the end of the near field domain in TAMOC. The random walk and displacement histograms show much more variability with depth, with Koh and Fan (1970)'s solution having remaining particles in the upper 16 meters and Broecker

and Peng (1982)'s solution having remaining particles in the upper 13 meters. Both solutions provide similar results with vertical mixing present throughout the entire shallow depth.

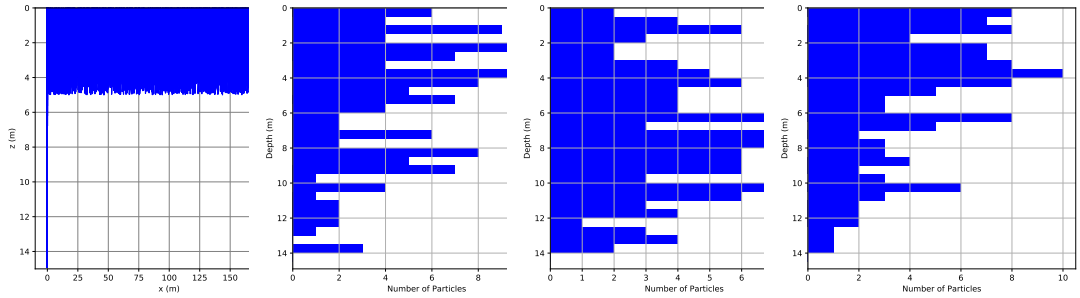

(a) TAMOC Advection Plume (b) Random Walk (c) RD(Koh and Fan, 1970) (d) RD(Broecker and Peng, 1982)

Figure 5.17: ADAC Scenario 2 - TAMOC Results

In Figure 5.18, both graphs are displaying random displacement. Kullenberg (1971)'s solution assumes the entire depth of the water column due to the shallow depth. The oil particles are approximately, evenly distributed among the entire water column representing the effect of wind forcing in a shallow water. The increase in wind speed shows a more vertically and evenly mixed profile, indicating an increase in vertical mixing.

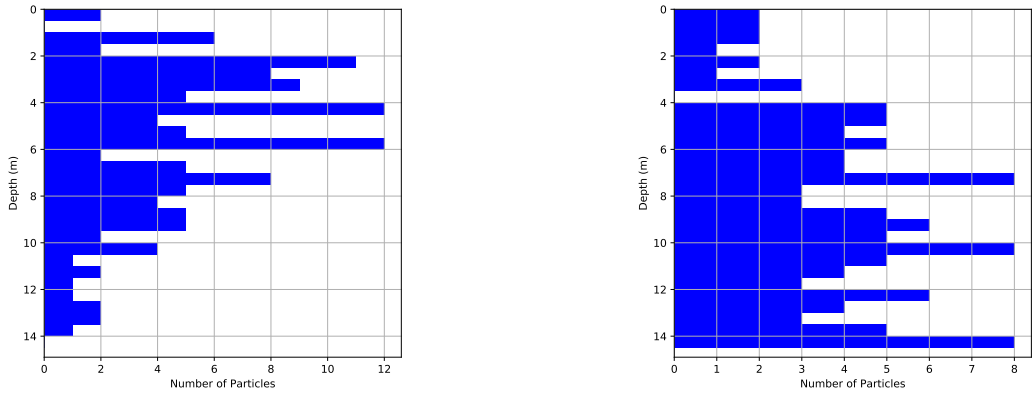

(a) 5 m/s Wind (b) 15 m/s Wind

Figure 5.18: ADAC Scenario 2 - TAMOC Results with Wind

We coupled TAMOC with GNOME to compute a farfield trajectory and continued to run the model one day after oil spill release duration. The results for Scenario 2 are shown in the following figures:

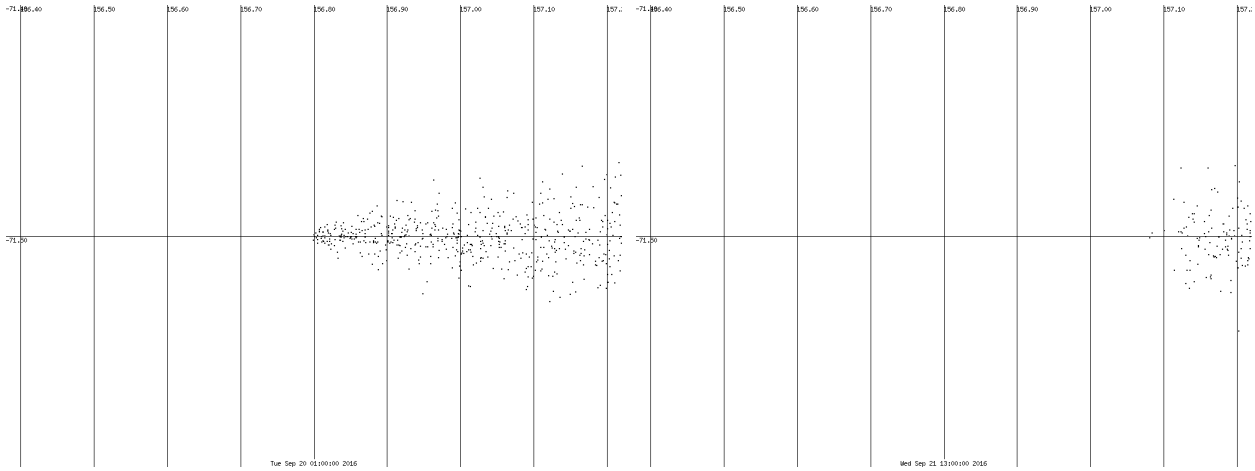

(a) Elapsed time: 1 day (b) Elapsed time: 2 days

Figure 5.19: Scenario 2 - Pure Advection

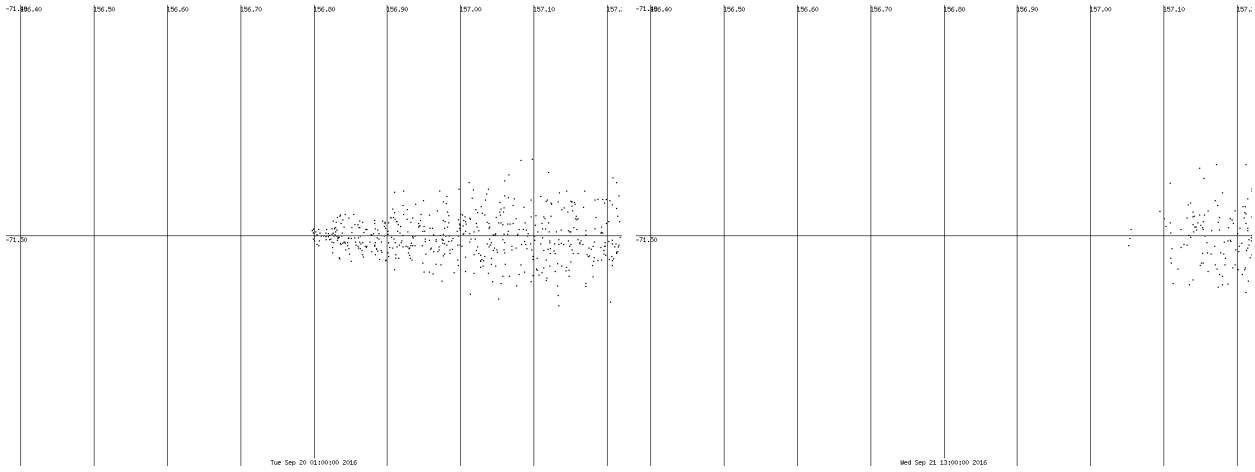

(a) Elapsed time: 1 day (b) Elapsed time: 2 days

Figure 5.20: Scenario 2 - Random Walk

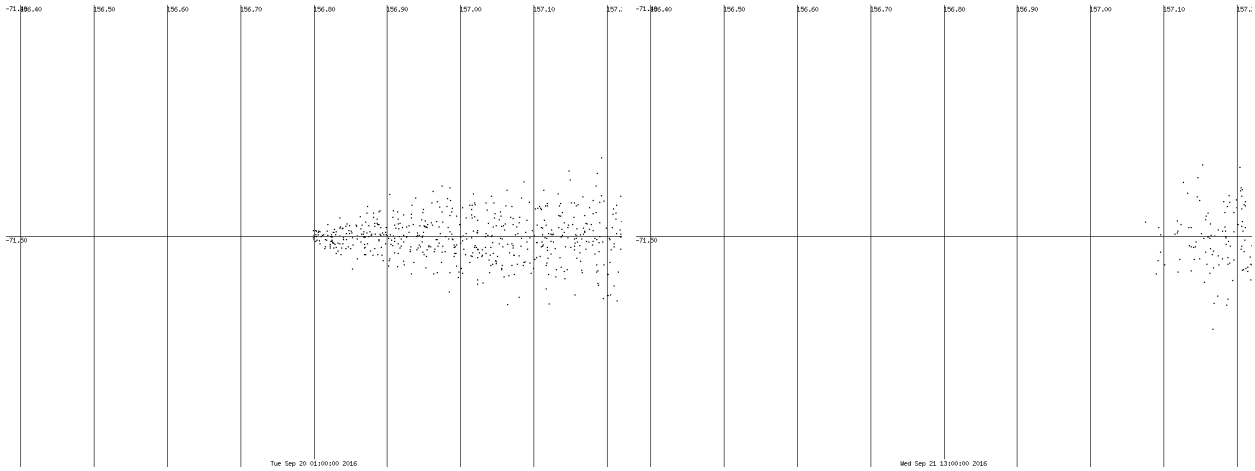

(a) Elapsed time: 1 day (b) Elapsed time: 2 days

Figure 5.21: Scenario 2 - Random Displacement (Koh and Fan, 1970)

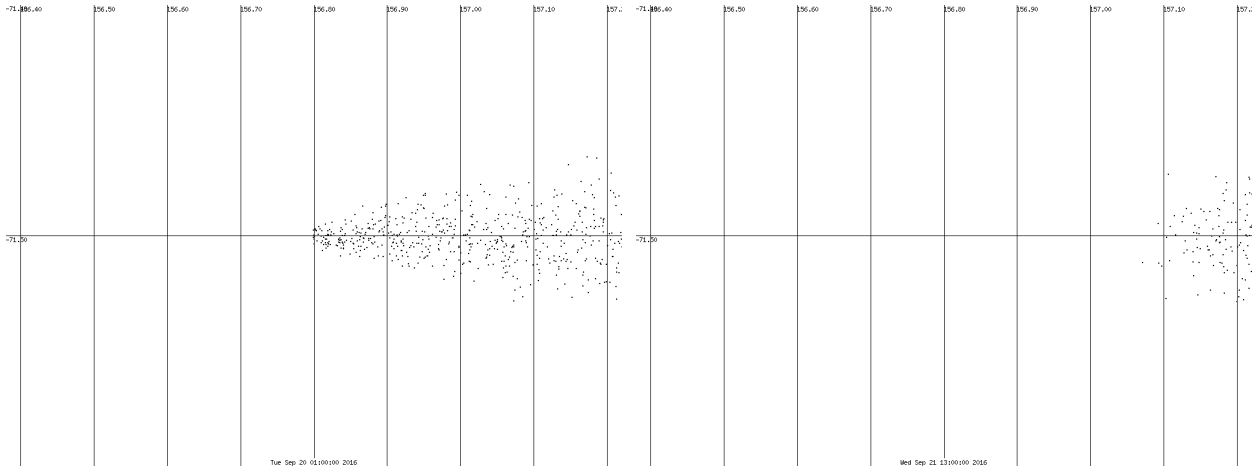

(a) Elapsed time: 1 day (b) Elapsed time: 2 days

Figure 5.22: Scenario 2 - Random Displacement (Broecker and Peng, 1982)

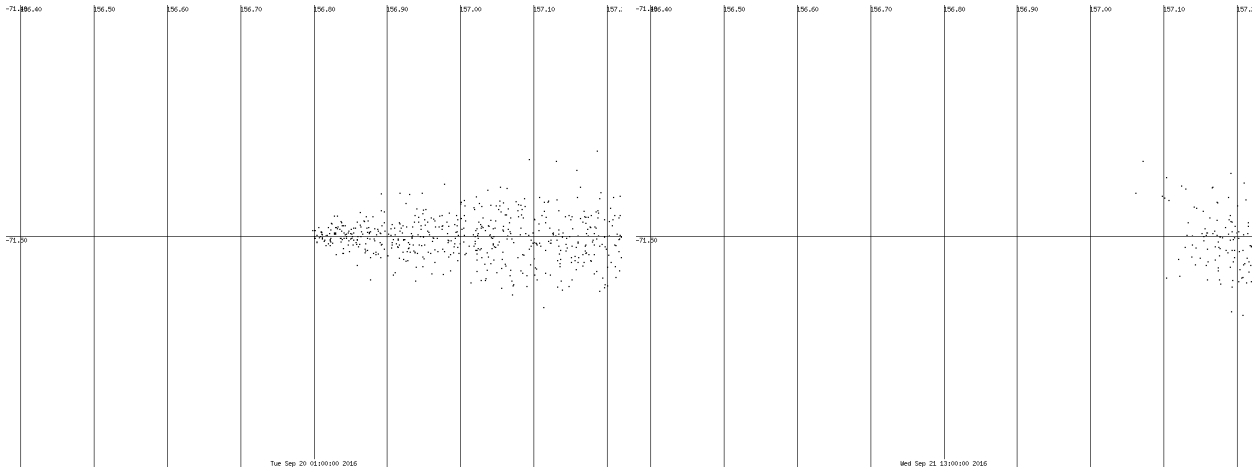

(a) Elapsed time: 1 day, Wind = 5 m/s (b) Elapsed time: 2 days, Wind = 5 m/s

Figure 5.23: Scenario 2 - Random Displacement (Broecker and Peng, 1982; Kullenberg, 1971)

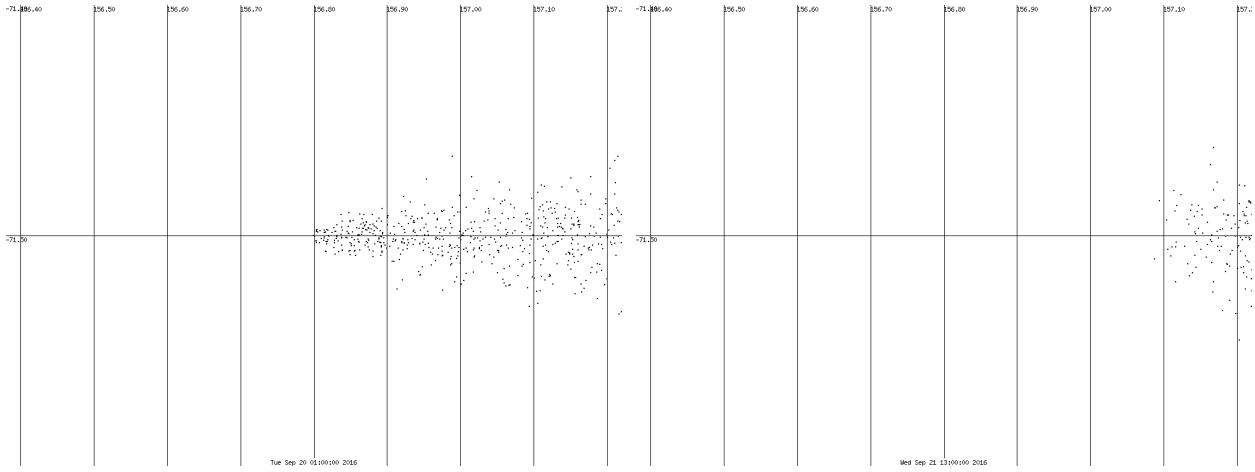

(a) Elapsed time: 1 day, Wind = 5 m/s (b) Elapsed time: 2 days, Wind = 5 m/s

Figure 5.24: Scenario 2 - Random Displacement (Koh and Fan, 1970; Kullenberg, 1971)

The GNOME output from Scenario 2 demonstrates the added diffusion to an oil trajectory with a horizontal current velocity. The output with pure advection, Figure 5.19, shows a concentrated spill close to the release location with little deviation in particle paths. After 1 day, the random displacement graphs show expected results for diffusive transport, depicting a wider surface area and particles scattered further apart with random motion.

5.4 ADAC Scenario 3: Burger Well Blowout

ADACE Scenario 3 simulates a well blowout of gas and oil. ADAC Scenario 3 has the following TAMOC spill parameters:

Table 5.4: "Scenario3.py" Inputs for TAMOC - Oil Spill

Parameter	Input
release_time	datetime(2017, 04, 04, 12, 0)
start_position	(-148.7, 71.5, 14.9)
end_release_time	start_time + timedelta(days=2)
diameter	0.254 m
release_temp	310.37 K
release_phi	$-\pi/2$
release_theta	0 rad
release_flowrate	10,000 barrels per day
discharge_salinity	0 psu
tracer_concentration	1
hydrate	True
dispersant	False
sigma_fac	np.array([[1.], [1. / 200.]])
inert_drop	False
d50_gas	0.008 m
d50_oil	0.0038 m
nbins	20
ua	0.14 m/s

The TAMOC results for comparing the differences in vertical location between pure advection, random walk, and random displacement applications are displayed in Figure 5.25 and Figure 5.26. These figures show the differences in vertical locations at the end of the near field domain in TAMOC. The random displacement histograms show much more variability with depth, with Koh

and Fan (1970)'s solution having remaining particles in the upper 5 meters and Broecker and Peng (1982)'s solution having remaining particles in the upper 7 meters.

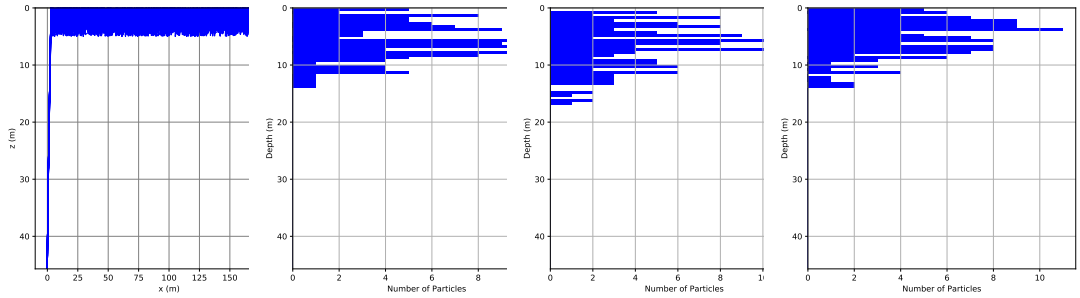

(a) TAMOC Advection Plume (b) Random Walk (c) RD(Koh and Fan, 1970) (d) RD(Broecker and Peng, 1982)

Figure 5.25: ADAC Scenario 3 - TAMOC Results

In Figure 5.26, both graphs are displaying random displacement. Kullenberg (1971)'s solution assumes the entire depth of the water column due to the shallow depth. The oil particles are approximately, evenly distributed among the entire water column representing the effect of wind forcing in a shallow water.

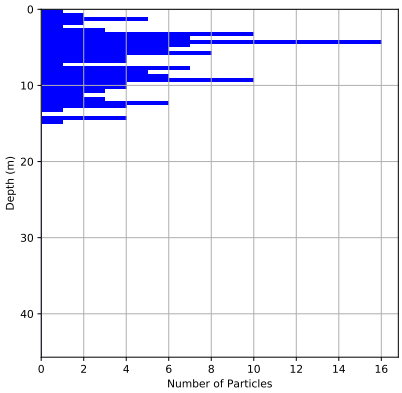

(a) 5 m/s Wind

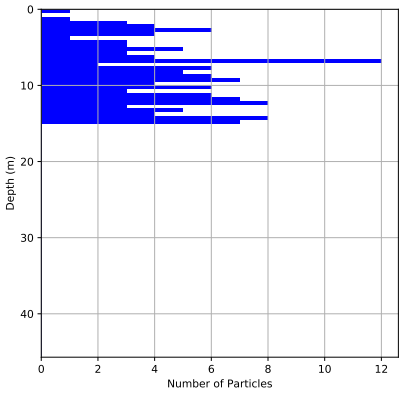

(b) 15 m/s Wind

Figure 5.26: ADAC Scenario 3 - TAMOC Results with Wind

The majority of the TAMOC output graphs show a general trend of particle accumulation towards the surface, this is caused by the application of the slip velocity in the advection scheme which is a positive force towards the ocean surface.

We coupled TAMOC with GNOME to compute the farfield trajectory. The results for Scenario 3 are shown in the following figures:

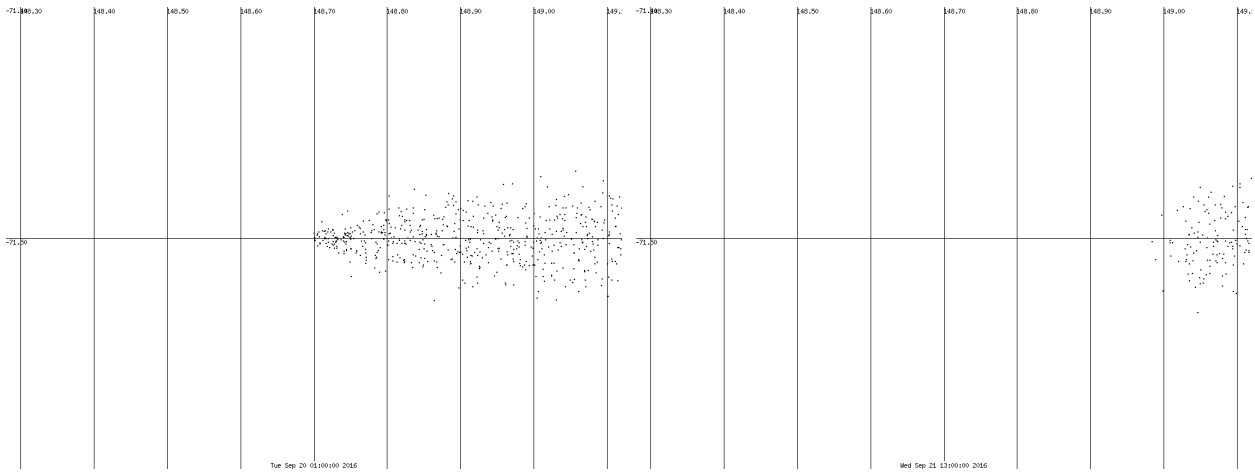

(a) Elapsed time: 1 day

(b) Elapsed time: 2 days

Figure 5.27: Scenario 3 - Pure Advection

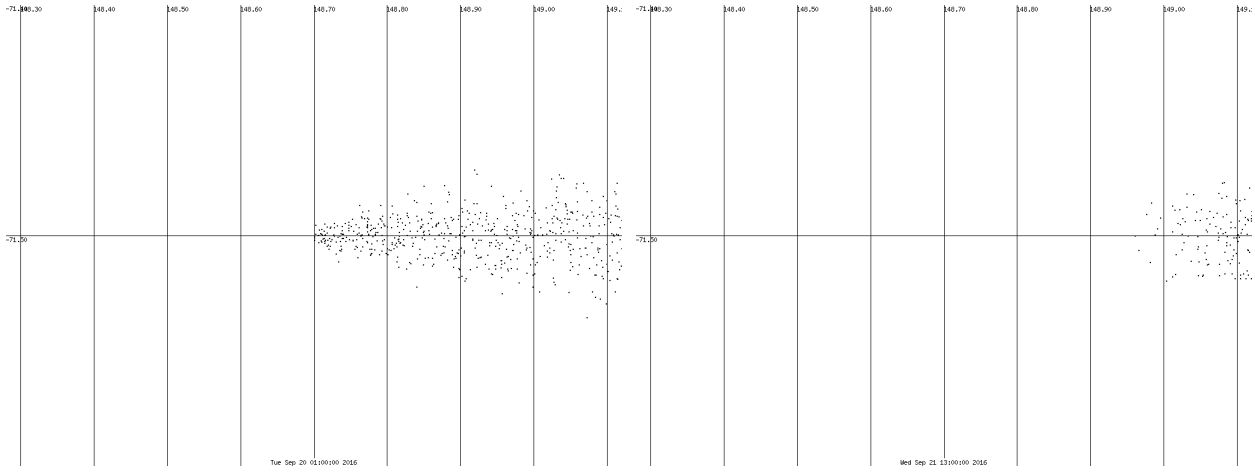

(a) Elapsed time: 1 day (b) Elapsed time: 2 days

Figure 5.28: Scenario 3 - Random Walk

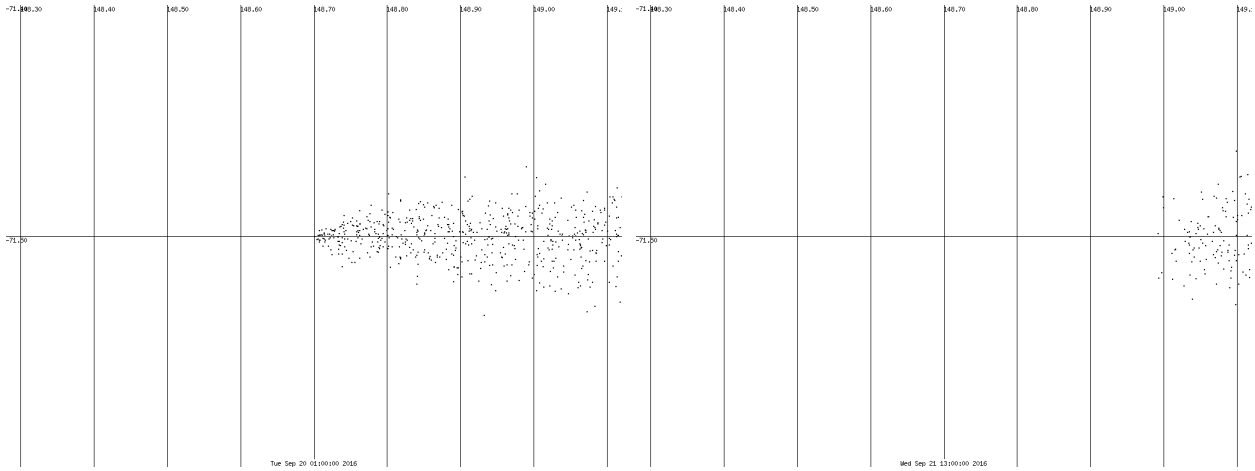

(a) Elapsed time: 1 day (b) Elapsed time: 2 days

Figure 5.29: Scenario 3 - Random Displacement (Koh and Fan, 1970)

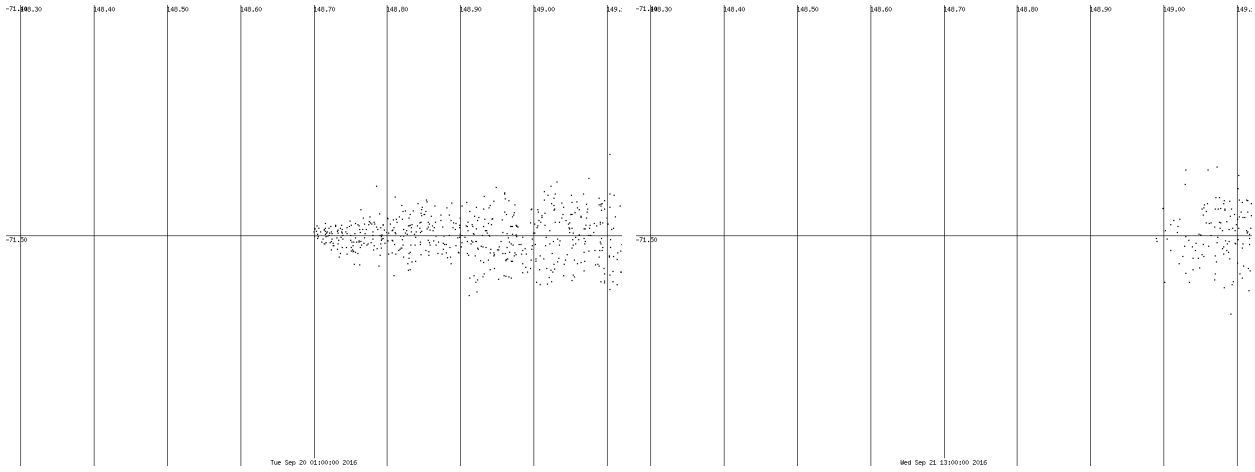

(a) Elapsed time: 1 day (b) Elapsed time: 2 days

Figure 5.30: Scenario 3 - Random Displacement (Broecker and Peng, 1982)

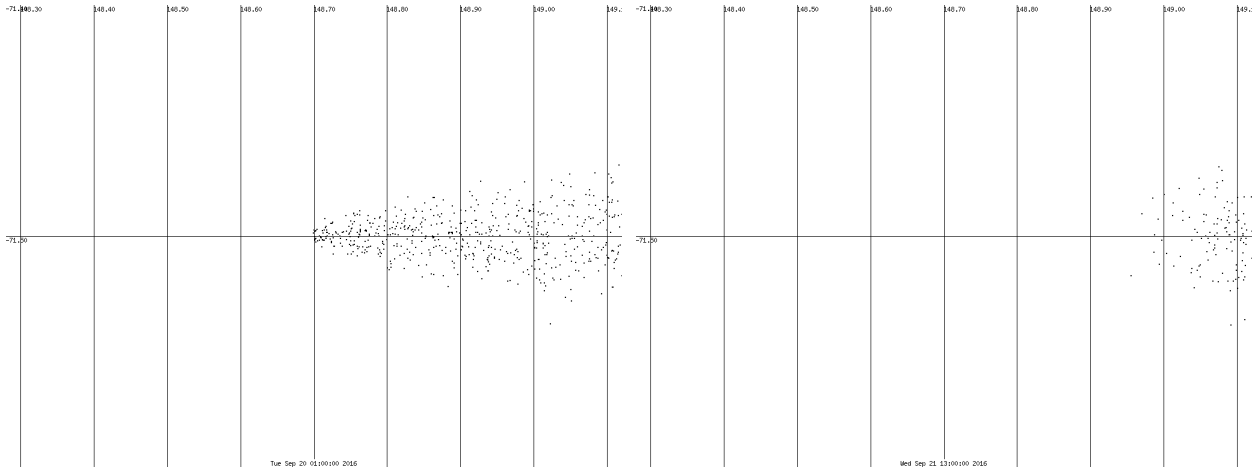

(a) Elapsed time: 1 day, Wind = 5 m/s (b) Elapsed time: 2 days, Wind = 5 m/s

Figure 5.31: Scenario 3 - Random Displacement (Broecker and Peng, 1982; Kullenberg, 1971)

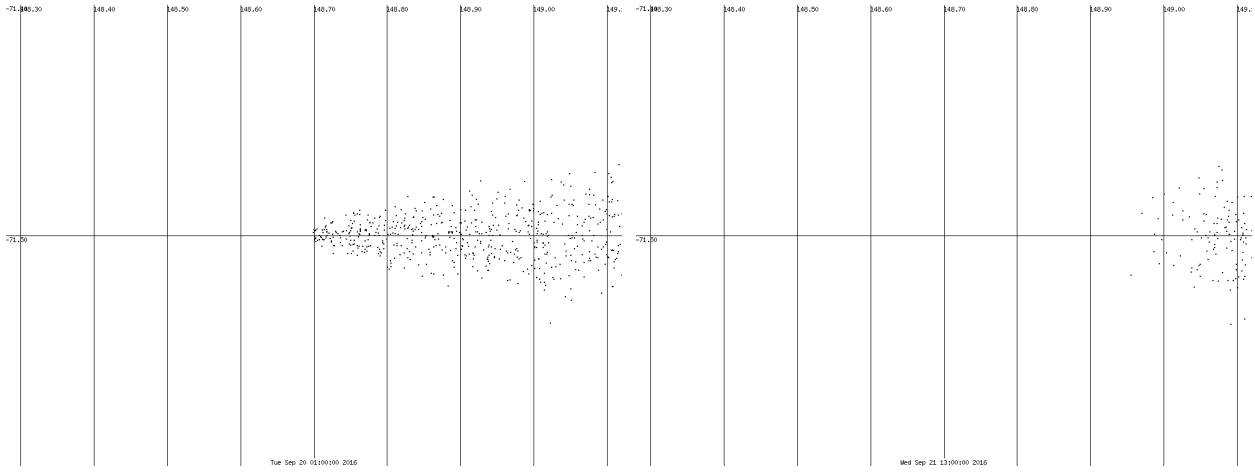

(a) Elapsed time: 1 day, Wind = 5 m/s (b) Elapsed time: 2 days, Wind = 5 m/s

Figure 5.32: Scenario 3 - Random Displacement (Koh and Fan, 1970; Kullenberg, 1971)

The GNOME output from Scenario 3 demonstrates the added diffusion to an oil trajectory with a horizontal current velocity. The output with pure advection, Figure 5.27, shows a concentrated spill close to the release location with little deviation in particle paths. After 1 day, the random displacement graphs show expected results for diffusive transport, depicting a wider surface area and particles scattered further apart with random motion. Random individual particles can be seen in the random displacement graphs like Figures 5.29 and 5.30, a much wider surface area is shown in Figures 5.31 and 5.32 with respect to the surface area shown in the pure advection figure, Figure 5.27.

6. RECOMMENDATIONS

6.1 Further Platform Modifications

Further modifications to simplify the model coupling method is important to improve the functionality of TAMOC-GNOME coupling. A central location to input which transport model to use, the diffusivity profile, the maximum range to compute, the maximum time to compute, and the specific spill parameters is ideal. The result of these modifications would ensure an accessible, modifiable, and efficient resource for predicting oil spill trajectory.

Future modifications to the TAMOC model will include a more accurate calculation of vertical diffusivity. This thesis conducted the first step in successfully applying diffusion to the model, so empirical diffusion relationships were appropriate. Moving forward with the TAMOC model with diffusion, the possible implementation of the General Ocean Turbulence Model (GOTM) is considerable to define a diffusivity profile for a given density and stratification profile. Utilizing GOTM within the TAMOC model to define a turbulent diffusivity profile from it's one-point turbulence modeling scheme is a strong possibility due to the detailed GOTM output which is capable of wind input and provides a more accurate diffusivity profile for wind and wave data versus an empirical solution.

6.2 Further Research

Additional research into the role waves has in the vertical mixing of surfaced oil would be beneficial. In this thesis, surfaced particles are resuspended randomly within the upper mixed ocean layer in order to simulate wind and wave breaking or Langmuir circulations. In order to further accurately assess the affect of waves on a surfaced oil spill, this model needs to consider Stokes drift which calculates the particle movement in the direction of wave propagation. Some oil spill models approximate Stokes drift from wind drift, where a percentage of the wind drift is applied at an angle of the wave direction (Le Hénaff et al., 2012). There has been research conducted which shows Stokes drift can have a significant impact on the fate of an oil spill which

means Stokes drift should be considered in the future to ensure accuracy with TAMOC model simulations (Le Hénaff et al., 2012).

Field data for arctic spills would be useful in further validating the effects of advection and diffusivity in adverse conditions. Enhanced background knowledge of regional environmental conditions such as local diffusion coefficients and salinities would be highly beneficial to understanding and applying diffusive transport appropriately. Researching and improving methods for defining mixed layer depths and vertical diffusivity relationships with wind in order to compare output and reliability. Once diffusivity has been properly validated with field data and other models, future work would consist of applying the random displacement scheme in GNOME and coupling with a TAMOC spill. A hybrid model for nearfield and farfield plume effects, considering weathering processes, entrainment, dispersion, and ice, is critical for predicting a realistic fate of an oil spill in the Arctic.

7. CONCLUSIONS

An oil spill model for predicting oil spill trajectories with random displacement diffusion was developed and validated in Python. The oil spill model was built upon the previously developed model, Texas A&M Oil Spill Calculator (TAMOC), by Socolofsky et al. (2008). This model uses empirical solutions for vertical, turbulent diffusion by Broecker and Peng (1982), Koh and Fan (1970), and Kullenberg (1971). The diffusive oil particle trajectory was calculated using a random displacement model defined in Visser (1997), with the assumption that surfaced particles reflect back into the water column randomly within a defined mixed layer depth. The model uses Lagrangian particle tracking to track particles inside and outside a subsurface oil spill plume in a nearfield domain and the output is sent to the National Oceanographic and Atmospheric Administration (NOAA)'s farfield oil spill model, General NOAA Operational Modeling Environment (GNOME). The final spill location was derived from the nearfield plume output from TAMOC and the farfield calculation from GNOME where environmental elements are modified in either or both models to simulate realistic oil spill trajectory.

The following objectives were completed in this thesis: conduct extensive literature review, create a diffusivity-capable oil spill calculator, apply different empirical relationships for diffusivity and compare, and couple oil spill calculator with GNOME. The model created is operational within 2-3 hours varying with the defined nearfield range and empirical diffusivity solutions for deep water, shallow water, and wind which can be selected to cater each scenario. The mixed layer depth is determined using a threshold for difference in potential density and surfaced particles are reflected back into the mixed layer depth randomly.

The model projection varied greatly between pure advection and added diffusion simulations as expected. The TAMOC output of the vertical particle distribution was compared for each diffusion solution versus pure advection and random walk. When adding a diffusive transport, we expose the particles to turbulent eddies or vertical mixing which causes the particles to deviate from the spill's center of mass and travel further vertically than they would under pure advection. The

model results for all cases correlated with this theory. The diffusivity output from the empirical relationships were within expected diffusivity values and the application by random displacement was validated by pushing neutrally buoyant particles through the scheme and ensuring a similar distribution after a specified time. The GNOME output images show greater concentrations where vertical diffusivity is applied but did not have a large impact on the overall position of the spill in the farfield domain. The application of vertical diffusion transport proved to be successful in the model shown by the larger variation of vertical particles due to the random motions added to advection in the transport module by random walk and random displacement.

Diffusive transport plays an important role within an oil spill trajectory model, without diffusion applied an oil spill model can under predict the extent an oil spill will travel. In addition, using random displacement has been proven more accurate than random walk due to the varying diffusivity profiles commonly found in the ocean. The modeling of diffusive transport can now be applied to the fate of an oil spill in TAMOC. TAMOC's diffusivity solutions require further validation with field data, but it is the first step to improving the model's transport scheme.

REFERENCES

ABSG Consulting Inc. (2018). *US Outer Continental Shelf Oil Spill Statistics*.

Alaska Department of Environmental Conservation (2015). *Annual Summary of Oil and Hazardous Substance Spills*.

Broecker, W. S. and Peng, Z. (1982). *Tracers in the sea*. Palisades, N.Y. : Lamont-Doherty Geological Observatory, Columbia University.

Burchard, H. and Baumert, H. (1995). On the performance of a mixed-layer model based on the κ-ϵ turbulence closure. *Journal of Geophysical Research-Oceans*, 100(C5):8523–8540.

Bureau of Ocean Energy Management (2018). *2017 Assessment of Undiscovered Oil and Gas Resources in the Western Beaufort Sea OCS Planning Area*.

Canuto, V. M., Howard, A., Cheng, Y., and Dubovikov, M. S. (2002). Ocean turbulence. part ii: Vertical diffusivities of momentum, heat, salt, mass, and passive scalars. *Journal of Physical Oceanography*, 32(1):240–264.

Csanady, G. T. (1973). *The Fluctuation Problem in Turbulent Diffusion*, pages 222–248. Geophysics and Astrophysics Monographs, An International Series of Fundamental Textbooks: 3. Dordrecht : Springer Netherlands.

Díaz, B., Pavón, A., and Gómez-Gesteira, M. (2008). Use of a probabilistic particle tracking model to simulate the prestige oil spill. *Journal of Marine Systems*, 72(1):159 – 166.

Dissanayake, A. L., Gros, J., and Socolofsky, S. A. (2018). Integral models for bubble, droplet, and multiphase plume dynamics in stratification and crossflow. *Environmental Fluid Mechanics*, 18(5):1167–1202.

Dominicis, M. D., Pinardi, N., Zodiatis, G., and Lardner, R. (2013). Medslik-ii, a lagrangian marine surface oil spill model for short-term forecasting - part 1: Theory. *Geoscientific Model Development*, 6:1851–1869.

Gräwe, U. (2011). Implementation of high-order particle-tracking schemes in a water column model. *Ocean Modelling*, 36:80 – 89.

Gros, J. and Socolofsky, S. (2017). Simulation of scenarios of subsea accidental releases of oil and gas in alaska.

Gros, J., Socolofsky, S. A., Dissanayake, A. L., Jun, I., Zhao, L., Boufadel, M. C., Reddy, C. M., and Arey, J. S. (2017). Petroleum dynamics in the sea and influence of subsea dispersant injection during deepwater horizon. *Proceedings of the National Academy of Sciences*.

Holloway, G. (1994). Comment: on modelling vertical trajectories of phytoplankton in a mixed layer. *Deep Sea Research Part I: Oceanographic Research Papers*, 41(5):957–959.

Hunter, J., Craig, P., and Phillips, H. (1993). On the use of random walk models with spatially variable diffusivity. *Journal of Computational Physics*, 106(2):366–376.

ITOPF (2019). Oil spill modelling.

J. Thomson, D. (1984). Random walk modelling of diffusion in inhomogeneous turbulence. *Q.J.R. Meteorological Society*, 110:1107–1120.

Johansen, Ø. (2000). Deepblow - a lagrangian plume model for deep water blowouts. *Spill Science & Technology Bulletin*, 6(2):103 – 111.

Kileso, A., Chubarenko, B., Zemlys, P., and Kuzmenko, I. (2014). Oil spill modelling methods: application to the south-eastern part of the baltic sea. *Baltica*, 27:15–22.

Koh, R. C. Y. and Fan, L.-N. (1970). *Mathematical models for the prediction of temperature distributions resulting from the discharge of heated water into large bodies of water*. U.S. Gov. Printing Office.

Kullenberg, G. (1971). Vertical diffusion in shallow waters. *Tellus*, 23(2):129–135.

Le Hénaff, M., Kourafalou, V. H., Paris, C. B., Helgers, J., Aman, Z. M., Hogan, P. J., and Srinivasan, A. (2012). Surface evolution of the deepwater horizon oil spill patch: Combined effects of circulation and wind-induced drift. *Environmental Science & Technology*, 46(13):7267–7273.

Matsuzaki, Y. and Fujita, I. (2014). Horizontal turbulent diffusion at sea surface for oil transport simulation. *Coastal Engineering Proceedings*, 1(34):8.

Okubo, A. (1986). Dynamical aspects of animal grouping: Swarms, schools, flocks, and herds. *Advances in Biophysics*, 22:1 – 94.

Press, W. H., Teukolsky, S. A., Vetterling, W. T., and Flannery, B. P. (2007). *Numerical Recipes 3rd Edition: The Art of Scientific Computing*. Cambridge University Press, New York, NY, USA, 3 edition.

Reed, M., Johansen, Ø., Brandvik, P. J., Daling, P., Lewis, A., Fiocco, R., Mackay, D., and Prentki, R. (1999). Oil spill modeling towards the close of the 20th century: Overview of the state of the art. *Spill Science & Technology Bulletin*, 5(1):3–16.

Schneider, N. and Müller, P. (1990). The meridional and seasonal structures of the mixed-layer depth and its diurnal amplitude observed during the hawaii-to-tahiti shuttle experiment. *Journal of Physical Oceanography*, 20(9):1395 – 1404.

Sinha, N. and Golshan, R. (2018). Material transport under a wave train in interaction with constant wind: A eulerian rans approach combined with a lagrangian particle dispersion model. *Fluids*, 3:40.

Socolofsky, S. A., Bhaumik, T., and Seol, D.-G. (2008). Double-plume integral models for near-field mixing in multiphase plumes. *Journal of Hydraulic Engineering*, 134(6):772–783.

Socolofsky, S. A., Dissanayake, A. L., Jun, I., Gros, J., Arey, J. S., and Reddy, C. M. (2015). Texas a&m oilspill calculator (tamoc): Modeling suite for subsea spills.

Spaulding, M. L. (2017). State of the art review and future directions in oil spill modeling. *Marine Pollution Bulletin*, 115(1):7–19.

Taylor, G. I. (1921). Diffusion by continuous movements. *Proceedings of the London Mathematical Society*, 20(1):196–212.

Thomson, R. E. and Fine, I. V. (2003). Estimating mixed layer depth from oceanic profile data. *Journal of Atmospheric & Oceanic Technology*, 20(2):319.

U.S. National Commission on the BP Deepwater Horizon Oil Spill and Offshore Drilling (2011). *Deep water : the Gulf oil disaster and the future of offshore drilling : report to the President. National Commission on the BP Deepwater Horizon Oil Spill and Offshore Drilling.*

Visser, A. W. (1997). Using random walk models to simulate the vertical distribution of particles in a turbulent water column. *Marine Ecology Progress Series*, page 275.

Wegener, M., Paul, N., and Kraume, M. (2014). Fluid dynamics and mass transfer at single droplets in liquid/liquid systems. *International Journal of Heat and Mass Transfer*, 71:475 – 495.

Young, W. R., Rhines, P. B., and Garrett, C. J. R. (1982). Shear-flow dispersion, internal waves and horizontal mixing in the ocean. *Journal of Physical Oceanography*, 12(6):515–527.

Zelenke, B., O'Connor, C., Barker, C., Beegle-Krause, C. J., and Eclipse, L. (2012). General noaa operational modeling environment (gnome) technical documentation. Technical report, Emergency Response Division, NOAA.

Zheng, L. and Yapa, P. D. (1998). Simulation of oil spills from underwater accidents ii: Model verification. *Journal of Hydraulic Research*, 36(1):117–134.